Genomic landscape of early ecological speciation initiated by selection on nuptial color

David Alexander MARQUES (DAM)[1,2,*], Kay LUCEK (KL)[1,2,3], Marcel Philipp HAESLER (MPH)[1,2], Anna Fiona FELLER (AFF)[1,2], Joana Isabel MEIER (JIM)[1,2], Catherine Elise WAGNER (CEW)[1,2,4], Laurent EXCOFFIER (LE)[1,5] & Ole SEEHAUSEN (OS)[1,2]

[1]Institute of Ecology & Evolution, University of Berne, Switzerland; [2]Eawag: Swiss Federal Institute of Aquatic Science and Technology, Kastanienbaum, Switzerland; [3]University of Sheffield, UK; [4]Biodiversity Institute, University of Wyoming, USA; [5]Swiss Institute of Bioinformatics, Lausanne, Switzerland.

Keywords: sympatric divergence, ecological speciation, sexual selection, threespine stickleback, genomic islands

*Corresponding Author: David Alexander Marques, Baltzerstrasse 6, CH-3012 Bern, Switzerland, +41 31 631 3016, david.marques@iee.unibe.ch

Running title (<45 characters): Genomics, nuptial color & ecological speciation

Abstract

Ecological speciation is the evolution of reproductive isolation as a consequence of direct divergent natural selection or ecologically mediated divergent sexual selection. While the genomic signature of the former has been extensively studied in recent years, only few examples exist for genomic differentiation where environment-dependent sexual selection has played an important role. Here, we describe a very young (~90 years old) population of threespine sticklebacks exhibiting phenotypic and genomic differentiation between two habitats within the same pond. We show that differentiation among habitats is limited to male throat color and nest type, traits known to be subject to sexual selection. Divergence in these traits mirrors divergence in much older benthic and limnetic stickleback species pairs from North American Westcoast lakes, which also occur in sympatry but are strongly reproductively isolated from each other. We demonstrate that in our population, differences in throat color and breeding have been stable over a decade, but in contrast to North American benthic and limnetic stickleback species, these mating trait differences are not accompanied by divergence in morphology related to feeding, predator defense or swimming performance. Using genome-wide SNP data, we find multiple genomic islands with moderate differentiation spread across several chromosomes, whereas the rest of the genome is undifferentiated. The islands contain potential candidate genes involved in visual perception of color. Our results suggest that phenotypic and multi-chromosome genomic divergence of these morphs was driven by environment-dependent sexual selection, demonstrating incipient speciation after only a few decades of divergence in sympatry.

Introduction

Ecological speciation, the evolution of reproductive isolation between groups of individuals due to adaptation to different environments (Rundle & Nosil 2005), has received much attention in the last decade. However, the contributions of different evolutionary forces to the initiation and completion of speciation, their interactions and the chronology in which they operate are not yet well understood. The rise of the genomics era has come with much promise in particular for ecological speciation research (Rice *et al.* 2011; Nosil 2012; Seehausen *et al.* 2014), as targets of divergent selection can be detected at the genome level and insight into the genomic architecture of traits and genomic differentiation may unravel some of the mysteries about why some populations split and others do not, and why some lineages speciate more often or more rapidly than others. Consequently, many putative cases of ecological speciation have recently been the subject of genomic study, but most of these either are allopatric or parapatric ecotypes that do not persist in real sympatry (Soria-Carrasco *et al.* 2014) or of species pairs that do persist in sympatry but are already thousands to millions of generations divergent (Jones *et al.* 2012a; Nadeau *et al.* 2012; Renaut *et al.* 2013; Arnegard *et al.* 2014; Malinsky *et al.* 2015). Many of the best documented late stages of ecological speciation with now sympatric species have likely undergone an extended allopatric phase (Jones *et al.* 2012a; Martin *et al.* 2013; Renaut *et al.* 2013), making it sometimes difficult to distinguish between effects of divergent selection and other processes affecting genomic differentiation because these species have complex histories with periods of strong isolation (Cruickshank & Hahn 2014). Until now only very few studies have characterized genomic differentiation in very young sympatric forms that exchange genes (Michel *et al.* 2010; Malinsky *et al.* 2015).

The early stage of ecological speciation, i.e. when divergent or disruptive natural or environment-dependent sexual selection are initiating reproductive isolation, is of particular interest because barriers reducing gene flow early in the speciation process have a larger effect on the origin of reproductive isolation than late-acting barriers (Coyne & Orr 2004). Very early stages may, for instance, be needed to investigate the relative importance of divergent natural and sexual selection in

initiating divergence. This is because in most advanced stages of speciation both types of selection have already been acting and may have led to character divergence, making it impossible to tell how the process began (Maan & Seehausen 2011). The beginning of ecological speciation or 'incipient' speciation is thought to be accompanied by genomic divergence in multiple small genomic regions diverging despite gene flow (Wu 2001; Feder *et al.* 2012; Marques *et al.* 2016), a genomic signature of divergent selection reducing gene flow locally in the genome and therein causing 'isolation by adaptation' (Nosil *et al.* 2008; Nosil 2012).

Here, we characterize a case of very recent phenotypic and genomic divergence in sympatry observed within a population of threespine stickleback (*Gasterosteus aculeatus* species complex) in a clear water pond, the Jordeweiher, near Bern, Switzerland. Stickleback have colonized the manmade Jordeweiher pond not more than 90 years ago. The population is now polymorphic for many traits that differ among sympatric limnetic and benthic stickleback species from lakes on the west coast of Canada (McPhail 1994; Vines & Schluter 2006), including nest type, breeding habitat, male throat color, body shape and size. This variation in phenotypic traits may have been facilitated by a hybrid origin of the population: The Jordeweiher was colonized by stickleback from an extensive hybrid zone between divergent stickleback lineages from Western, Northern and Eastern Europe that is situated in central Switzerland and formed within the last 150 years (Lucek *et al.* 2010; Roy *et al.* 2015). Jordeweiher stickleback (population 'EYM' in Roy *et al.* 2015) show the typical mitochondrial haplotype composition of Central Swiss populations, consisting of Rhine (Northern) and Baltic (Eastern) haplotypes (population 'EYM' in Roy *et al.* 2015; Lucek & Seehausen unpublished data). Additionally haplotypes from the Rhone lineage were found in Lake Wohlen just 1.5 km downstream from the Jordeweiher (Lucek *et al.* 2010).

Stickleback in this ~3,200 m^2 spring-fed clearwater pond build nests in two distinct but directly adjacent habitats that differ in multiple biotic and abiotic factors: 'offshore' habitat, the open, flat floor covered in fairly stable bot soft sediment of very light color (Fig. 1a), and 'nearshore' habitat, the steep clay bank below overhanging trees with increased structural complexity (branches, tree

roots, leaves, Fig. 1d). Besides substrate, slope and habitat complexity, the habitats also differ in light regime: offshore habitat receives direct and strong vertical sun light throughout most of the day and the sediment reflects brightly, while nearshore habitat is characterized by a more heterogeneous and dynamic light mosaic due to shade from overhanging trees, and the floor is covered in much darker leaf litter (Fig. 1a & d). Furthermore, the habitats may also differ in predator composition: only two avian predators have been recorded on the pond, none of which is likely to reach down to the bottom in the deeper offshore habitat, common kingfishers (*Alcedo atthis*) and grey herons (*Ardea cinerea*). Neither of them breeds in the nearest vicinity and they are thus only occasional visitors. The impoverished predator fauna is indeed a unique feature of the Jordeweiher compared to other stickleback habitats in Switzerland: only invertebrate predators such as large dragonfly larvae (suborder Anisoptera) are moderately abundant (Zeller *et al.* 2012), while a single northern pike (*Esox lucius*) was the only fish predator repeatedly observed in a single year. This low predation pressure could have allowed stickleback to colonize most of the available pond habitats, including the open pond with little shelter.

In 2007, OS discovered that variation in male nuptial color, body shape and nest morphology (an extended phenotype (Hunter 2009) shown by breeding males), may be associated with these habitats. This would be an example of multidimensional differentiation between phenotypes that may have evolved in sympatry, not known from stickleback anywhere else in central Europe. In this paper, we quantify phenotypic, ecological and genomic differentiation between males of the different color morphs and between males from different breeding habitats and we ask whether feeding-related, defense-related or sexual / social signaling traits are more strongly differentiated. We then investigate genomic differentiation and identify genomic islands diverging between male color morphs and between males from different habitats. Finally, we identify genomic candidate targets for divergent selection between color morphs and habitats. Based on the kind of traits showing phenotypic divergence between distinct breeding habitats, we infer the likely involvement of environment-dependent sexual selection. Thereby we aim to uncover the genomic landscape of very early

ecological speciation driven by environment-dependent sexual selection, which has not yet been studied in contrast to the genomics of ecological speciation largely driven by natural selection such as selection on resource use or predator avoidance.

Methods

Sampling site and collection

The Jordeweiher pond near Wohlen, Bern, Switzerland (46°57'24" N, 7°23'21" E) was built between 1901 and 1931 (Stengel & Lutz 1901; swisstopo 2015). We collected male stickleback from the pond in four different years: 2007 (June 12, n = 20), 2012 (May 6, n = 79), 2013 (July 18-23, n = 21) and 2015 (May 18-25, n = 20). In 2007 and 2012, we used minnow traps to collect fish, whereas in 2013 and 2015, we captured breeding males at their nests with hand nets while scuba diving. Upon capture, males were immediately photographed in a cuvette and subsequently anesthetized and euthanized using a clove oil solution, except for males in 2015, which were also tested in mate choice and nest site choice experiments (Feller *et al.* 2016). Fish capture and euthanasia was in accordance with the Swiss fisheries and veterinary legislation and granted permits issued by the cantonal veterinary office in Bern (permit numbers BE66/13, BE7/15) and by the owner of the Jordeweiher fishery rights (Augsburger AG, Hinterkappelen, Switzerland). In addition, between April and August 2008, we surveyed the population by snorkeling and photographing. We marked and mapped nest locations in the field in 2008 and triangulated and digitally mapped nest locations in 2013 and 2015 with QGIS v2.6.1 (QGIS Development Team 2015). We measured water depth at nest locations in 2013 and 2015 as well as the following nest characters for complete nests in 2013: diameter, slope, presence of assembled vegetation, presence and depth of depression and openness vs. concealment. Based on the slope and substrate where the stickleback built their nests, we classified the pond habitat into two breeding habitat categories: the 'offshore' habitat characterized by a thick layer of accumulated mud substrate and a flat topography (inclination < 15°), and the 'nearshore' habitat, characterized by clay-

like substrate without accumulating loose substrate but covered in leave litter and a steep topography (inclination > 15°, Fig. 3).

Color analysis

We measured male throat coloration from cuvette photographs taken in front of a neutral grey card. Males were photographed in ambient light in 2007 and 2012 and in standardized light from two external flashes in a black velour coated box in 2013 and 2015, using a Nikon E8700 in 2007 and a Canon EOS 7D in 2012-2015. Photographs were color-standardized in Photoshop Lightroom v3.6 (Adobe Inc.) using the neutral grey background for automatic white-balance adjustment and male throat coloration was measured in a 1 mm^2 circle without melanophores below the eye (Fig. S1) using ImageJ v1.49 (Schneider *et al.* 2012). The median red, blue and green (RGB) values from these sampled pixels were transformed into a median hue angle for each male (Preucil 1953; see also Feller *et al.* 2016), hereafter 'throat color'. Because not all males had attained their full nuptial colors in some years and because time in minnow traps may have caused males to lose color intensity in 2012 (Fig. 2c), one observer (DM) assigned the photographs to three nuptial coloration expression levels: 'fully colored' males showed excessive yellow to red coloration on throat and sides of the head up to the operculum, 'pale' males displayed the same distribution of colors as fully colored males, but with a lower intensity, while 'throat only' males showed coloration restricted to the lower throat, reflecting pre- or post-breeding condition.

We tested the distribution of throat color in the population for multimodality and assigned males to the respective modes using a cluster analysis based on a Gaussian mixture model implemented in the R-library *mclust* (Fraley & Raftery 2002). The *mclust* algorithm fits mixture models with varying numbers of normal mixture components to the data using the EM algorithm (Fraley & Raftery 2002). We assumed both equal and unequal variances for each mixture component, with equal variance models showing a better model fit judged by the Bayesian information criterion (BIC). We fitted up to three mixture components to the data and performed likelihood ratio tests (LRTs) to find the best

model, with significance estimated from 10’000 bootstrap LRT statistics. Based on the best fitting model, *mclust* assigned males to two clusters referred to as, a ‘red’ and an ‘orange’ cluster, corresponding to the two mixture components and hence the two modes in the throat color distribution.

We tested for a phenotype-environment association between breeding males’ throat color and breeding habitat. We first used throat hue angle and water depth at the nest (2013 and 2015 males only) in a linear mixed-effect model with color as response variable, depth as predictor variable and sampling year as random effect. To test for temporal stability of the throat color and habitat association, we included males from 2007 and 2012 and substituted depth by the binary ‘nearshore’ / ‘offshore’ habitat category in the linear mixed-effect model.

Linear and geometric morphometrics

We measured 17 standard linear morphological traits and placed 19 landmarks (Fig. S1) to study morphological variation among Jordeweiher stickleback males in linear and shape traits, using tpsDig v2.17 (Rohlf 2015), MorphoJ 1.06d (Klingenberg 2011) and custom R scripts. We size-corrected both linear and geometric morphometric data by extracting residuals from linear regressions of single traits and Procrustes coordinates respectively against standard length. We tested whether male breeding habitat and color morph can be predicted by morphometric distances or shape traits using linear mixed effect models, with traits as predictors and sampling year as random effects. We tested standard length, all size-corrected linear traits separately and combined into principal components (the five leading axes) as well as the first five principal components of overall shape, head and body shape and with false discovery rate adjusted p-values to assess significance of predictors. Following the approach by (Kaeuffer *et al.* 2012), we calculated P_{ST}, a scale-free estimator of phenotypic differentiation analogous to F_{ST}, for standard length, each size-corrected trait, for each of the first three principal components combining either all size corrected traits, feeding morphology, antipredator defense morphology or swimming performance traits (see Fig. S1 for grouping), and for

each of the three first principal components of shape traits (whole body, head and body shape respectively), between males grouped by color morph and by breeding habitat. By bootstrapping the data 1,000 times, we tested for significant differentiation among the groups, i.e. whether the 95% confidence interval for a P_{ST} exceeded zero, using bootstrap p-values adjusted for multiple testing using the false discovery rate method (Benjamini & Hochberg 1995).

Stomach content and stable isotope analyses

Stomach contents of stickleback collected in 2007 were analyzed under a dissecting microscope and we identified organisms in the diet to the level of order or family following (Lucek *et al.* 2012). We calculated the proportion of planktonic prey, i.e. the ratio of *Copepoda* plus *Cladocera* over the total number of food items. For stable isotope analysis, muscle tissue from the 2007 males was dried in an oven at 75°C for 48 h, pulverized, weighed to 0.25-0.28 mg packed into tin capsules and sent to the Environmental Isotope Laboratory (University of Waterloo, ON, Canada), as described in (Lucek *et al.* 2013). We tested whether male breeding habitat and color morph can be predicted by $\delta^{13}C$ and $\delta^{15}N$ isotope ratios or the percentage of planktonic prey using linear mixed effects models, with isotope ratios and planktonic prey proportion as predictors and sampling year as random effects. Analogous to P_{ST} outlined above, we calculated 'E_{ST}', a measure of ecological differentiation (Kaeuffer *et al.* 2012), for the percentage of planktonic prey and the $\delta^{13}C$ and $\delta^{15}N$ isotope ratios between male color morphs and breeding habitats and determined significance by bootstrapping the data 1,000 times.

Genomic data preparation

We sequenced 21 and 20 Jordeweiher males from 2013 and 2015 using the restriction-site associated DNA (RAD) sequencing protocol by Baird *et al.* (2008), with modifications described in Marques *et al.* (2016). Three RAD libraries were single-end sequenced on an Illumina HiSeq 2000 at the Next Generation Sequencing (NGS) Platform, University of Bern, Switzerland and the Center of Integrative Genomics (CIG), University of Lausanne, Switzerland. Each library was run on a single

lane together with other stickleback samples and 10% bacteriophage PhiX genomic DNA (Illumina Inc., San Diego CA, USA). The three libraries yielded 175, 188 and 142 million 100 bp long reads, respectively. We removed PhiX-reads from raw sequencing reads by alignment to the PhiX reference (accession: NC_001422; Sanger *et al.* 1977), de-multiplexed individuals and filtered for an intact *SbfI* restriction site using process_radtags v1.26 (Catchen *et al.* 2011). We aligned stickleback reads against a re-assembly of the stickleback genome (Glazer *et al.* 2015) using Bowtie 2 v2.2.6 (Langmead & Salzberg 2012) with default parameter end-to-end alignment. As described in (Marques *et al.* 2016), we recalibrated base quality scores using the PhiX-reads to empirically estimate sequencing error with the GATK v2.7 tools BaseRecalibrator and PrintReads (McKenna *et al.* 2010).

We called variants and genotypes simultaneously using the GATK tool UnifiedGenotyper (McKenna *et al.* 2010), with the following parameters: base quality score minimum 20, SNPs and indel genotype likelihood model, contamination rate 3%. Using vcftools v1.1.14 (Danecek *et al.* 2011) and custom python scripts, we removed sites with quality below 30, with more than 50% missing genotypes, indels and sites 3 bp up- or downstream of indels, SNPs with more than 2 alleles and individuals with more than 40% missing data. We also removed genotypes with quality below 30 and depth below 30 reads. Additionally, we excluded sites on the sex chromosome XIX from the dataset, due to uncertainty in mapping and variant calling, as no Y-chromosome reference is available for stickleback yet. Furthermore, we converted heterozygote genotypes with a strong read count imbalance for the two alleles, i.e. genotypes with less than 25% reads of the rarer allele, to homozygotes for the more common allele in order to prevent incorrect heterozygote calls due to potential PCR-induced errors. For the detection of genomic islands, we applied a minor allele frequency cut-off of 20% and computed F-statistics incorporating an inbreeding term, to prevent effects of potential erroneously called homozygotes due to PCR duplicates present in single-end RAD sequencing data (Baxter *et al.* 2011; Davey *et al.* 2011; Davey *et al.* 2013; Andrews & Luikart 2014; Puritz *et al.* 2014; Marques *et al.* 2016). We used custom bash and python scripts for filtering steps as well as PGDSpider v2.0.9.0 (Lischer & Excoffier 2012) for file conversion.

Population genomic analyses

We computed F-statistics (F_{ST}, F_{IT} and F_{IS}) for all Jordeweiher males grouped by color morph (orange vs. red) or breeding habitat (near- vs. offshore), using a locus-by-locus AMOVA as implemented in Arlequin v3.5.2.3 (Excoffier & Lischer 2010), allowing for within-individual variation and thus inbreeding. We ran 16,000 permutations to assess whether single locus F_{ST}'s are greater than zero, as suggested by Guoand Thompson (1992). In order to identify genomic islands of differentiation, defined here as genomic regions with an accumulation of loci with elevated differentiation, we used a Hidden Markov Model (HMM) approach (Hofer *et al.* 2012; Soria-Carrasco *et al.* 2014; Marques *et al.* 2016). First, we normalized F_{ST} values by transforming to $\log_{10}(F_{ST}+1)$ and applied an HMM with three normally distributed states to this series of transformed F_{ST} values, corresponding to 'genomic background' differentiation, 'low' and 'high' differentiation, the latter being 'genomic islands of differentiation' and referred to simply as 'genomic islands' from now onwards. Second, we retained genomic islands as such only if they contained loci with statistically significant differentiation after correction for multiple testing, as assessed based on p-values from AMOVA permutations corrected for a false discovery rate of 0.05, following (Sun & Cai 2009; Wei *et al.* 2009; Hofer *et al.* 2012).

In order to detect putative signatures of selection, we calculated nucleotide diversity in non-overlapping windows spanning multiple RAD-loci, so that a window contained at least 1,500 sequenced base pairs (max. 1,802 bp) without splitting RAD-loci across windows. We used only sites with maximal 50% missing data per group, grouped by color morph (orange vs. red) or breeding habitat (near- vs. offshore). This resulted in 1,823 and 1,825 windows for males grouped by habitat and color morph, respectively, spanning along chromosomes a mean distance of 217 kb (median 181 kb, range 37-1,773 kb) and 218 kb (median 192 kb, range 29-2,159 kb) respectively. We used Arlequin v3.5.2.3 (Excoffier & Lischer 2010) to estimate nucleotide diversity (π) for each group and window and calculated the differences in nucleotide diversity between groups ($\Delta\pi_{nearshore\text{-}offshore}$ and $\Delta\pi_{red\text{-}orange}$) for each window. We overlaid the positional information for genomic islands with these windows and assigned them accordingly to 'island windows' if they overlapped with genomic islands

or to 'genomic background windows' otherwise. We tested whether the absolute values of $\Delta\pi_{nearshore-offshore}$ and $\Delta\pi_{red-orange}$ of island windows were different from genomic background windows, using t-tests and false-discovery-rate adjusted p-values.

We overlaid positional information for genomic islands with those of Ensembl predicted genes (Jones *et al.* 2012b) and with previously identified quantitative trait loci (QTLs), candidate genes, expression outliers, and outlier regions (Peichel *et al.* 2001; Colosimo *et al.* 2004; Cresko *et al.* 2004; Shapiro *et al.* 2004; Colosimo *et al.* 2005; Kimmel *et al.* 2005; Coyle *et al.* 2007; Miller *et al.* 2007; Albert *et al.* 2008; Makinen *et al.* 2008a; Makinen *et al.* 2008b; Chan *et al.* 2009; Kitano *et al.* 2009; Chan *et al.* 2010; Hohenlohe *et al.* 2010; Kitano *et al.* 2010; DeFaveri *et al.* 2011; Greenwood *et al.* 2011; Shimada *et al.* 2011; Deagle *et al.* 2012; Greenwood *et al.* 2012; Jones *et al.* 2012a; Jones *et al.* 2012b; Kaeuffer *et al.* 2012; Malek *et al.* 2012; Rogers *et al.* 2012; Wark *et al.* 2012; Greenwood *et al.* 2013; Kitano *et al.* 2013; Arnegard *et al.* 2014; Berner *et al.* 2014; Cleves *et al.* 2014; Erickson *et al.* 2014; Glazer *et al.* 2014; Liu *et al.* 2014; Miller *et al.* 2014; Terekhanova *et al.* 2014; Yoshida *et al.* 2014; Conte *et al.* 2015; Ellis *et al.* 2015; Erickson *et al.* 2015; Feulner *et al.* 2015; Glazer *et al.* 2015; Greenwood *et al.* 2015; Guo *et al.* 2015; Roesti *et al.* 2015; Yong *et al.* 2015; Erickson *et al.* 2016; Marques *et al.* 2016). We tested whether the set of genes overlapping with genomic islands was enriched for gene ontology (GO) terms using the STRING v9.1 database (Franceschini *et al.* 2013) with a Bonferroni-corrected alpha level of 0.05. We also tested whether genomic islands fell more often into QTLs for 39 trait groups than expected by chance using a permutation approach (Marques *et al.* 2016). Genomic data analysis was performed using the bioinformatics infrastructure of the Genetic Diversity Centre (GDC), ETH Zurich/Eawag, on the Euler computer cluster at ETH Zurich and on the Ubelix computer cluster at University of Bern, Switzerland. Statistical analyses were conducted in R v3.2.2 (R Development Core Team 2015).

Results

Throat color polymorphism is stable and associated with the environment

Breeding males in the Jordeweiher pond show a bimodal distribution of throat color variation, with one mode of red-throated males and another mode of orange-throated males (Fig. 2a & b, LRT statistic=7.82, p=0.022). Red-throated males predominantly breed in the steep shore part of the pond, the 'nearshore' habitat, while orange-throated males mostly breed on the deeper and flatter bottom of the pond, the 'offshore' habitat (Fig. 3; males 2013 and 2015: $\beta_{\text{water depth at nest}}$=7.41, $t_{2,36}$=4.00, p<0.001, males 2007, 2012, 2013 and 2015, β_{habitat}=8.98, $t_{2,104}$=6.70, p<0.001). This association results in significant phenotypic differentiation between nearshore and offshore males for throat coloration (P_{ST}=0.37, p<0.001), Fig. 4). Furthermore, the association of male throat coloration with breeding habitat persisted over the surveyed period between 2007 and 2015 (Fig. 2c), demonstrating the temporal stability of this phenotype-environment association.

Weak differentiation in defense and feeding morphology and ecology

Besides throat coloration, morphological differentiation is weak between red and orange or nearshore and offshore breeding males: Red / nearshore males are slightly larger than orange / offshore males, have slightly larger heads and upper jaws, a shorter second spine and a longer dorsal fin as well as a deeper body (Tab. 1). However only swimming performance related trait differences (body depth and shape, dorsal fin length), predominantly among the color morphs, remain significant after correction for multiple testing (Tab. 1, Fig. S2 & S3). Concordantly, morphological differentiation is not significant in any of those traits after correction for multiple testing, neither between habitats nor between color morphs (Fig. 4).

Estimates of differentiation in feeding ecology among males breeding in different habitats (δ^{15}N E_{ST} = 0.11, δ^{13}C E_{ST} = 0.12, Fig. 4, Tab. 1) suggest a slight but not significantly increased carbon depletion in offshore-breeding males and an on average slightly elevated trophic position for nearshore males (Figs. 4 & S4). This trend is not present among color morphs. Weak differentiation in morphological traits is similar in direction between both habitats and color morphs, but slightly stronger among color morphs (standard length, body depth, swimming performance linear morphology), while ecological

differentiation estimates are higher between habitats than between color morphs (Fig. 4). The degree of differentiation in all these phenotypic and ecological traits is much lower than differentiation in throat coloration (Fig 4).

Genomic islands of differentiation

We studied patterns of genomic differentiation and diversity using a RAD sequencing derived dataset of 2,907,120 sequenced sites passing quality filters, including 11,733 SNPs, distributed across the genome. We computed relative differentiation (F_{ST}) for each SNP between male color morphs and between males breeding in the two different habitats, using a locus-by-locus AMOVA (see Methods). Averaged across all SNPs, mean genomic differentiation among nearshore and offshore breeding males (mean $F_{ST} = –0.0018$, permutation test $p > 0.05$) and red- and orange-throated males (mean $F_{ST} = –0.0010$, $p > 0.05$) is not significant and thus there is no genomic background differentiation among them. However, differentiation is heterogeneous across the genome, revealing a number of genomic regions with considerable differentiation ranging up to $F_{ST} = 0.46$ between color morphs and $F_{ST} = 0.48$ between breeding habitats (Fig. 5b & d). We used a Hidden Markov Model (HMM) approach and a subset of 7,669 SNPs with minor allele frequency > 20% to identify regions with an accumulation of differentiated loci. We found 14 such genomic islands of differentiation between red and orange stickleback males and 9 genomic islands between males grouped by breeding habitat (Fig. 5b & d, Table 2). Three genomic islands on chromosomes XII, XIV and XVIII are divergent both between males breeding in different habitats and males of the different color morphs.

In several genomic islands, nucleotide diversity is reduced in one of the two male types, indicative of habitat- or color morph-specific selective sweeps in those regions (Fig. 5a & c). For example island H.21b (Tab. 1, Fig. 5) shows a highly positive $\Delta\pi_{\text{nearshore-offshore}}$, suggesting a reduction of diversity due to a sweep in offshore males. In contrast, island HC.18 shows negative values for both $\Delta\pi_{\text{nearshore-offshore}}$ and $\Delta\pi_{\text{red-orange}}$ and thus reduced diversity in nearshore / red males, suggesting a selective sweep in nearshore/red males. Among males breeding in different habitats, island H.11 shows decreased

diversity in offshore males and island H.16 in nearshore males, while among red and orange males, islands C.2b and HC.12 show low diversity in orange males and island C.20d in red males (Fig. 5). Overall, differences in nucleotide diversity between nearshore vs. offshore males and red vs. orange males respectively were higher in genomic islands than in the genomic background (mean island $|\Delta\pi_{nearshore\text{-}offshore}| = 3.5 * 10^{-4}$, mean background $|\Delta\pi_{nearshore\text{-}offshore}| = 2.2 * 10^{-4}$, $t_{2,45} = -2.66$, $p = 0.011$; mean island $|\Delta\pi_{red\text{-}orange}| = 3.4 * 10^{-4}$, mean background $|\Delta\pi_{red\text{-}orange}| = 2.1 * 10^{-4}$, $t_{2,60} = -3.17$, $p < 0.001$). At the same time, raw estimates of nucleotide diversity are not lower in genomic islands than in the genomic background, neither within individuals grouped by habitat (mean island $\pi_{nearshore} = 1.37 * 10^{-3}$, mean background $\pi_{nearshore} = 1.41 * 10^{-3}$, $t_{2,47} = -0.31$, $p = 0.753$, mean island $\pi_{offshore} = 1.40 * 10^{-3}$, mean background $\pi_{offshore} = 1.38 * 10^{-3}$, $t_{2,48} = -0.20$, $p = 0.84$) nor by color morph (mean island $\pi_{red} = 1.38 * 10^{-3}$, mean background $\pi_{red} = 1.49 * 10^{-3}$, $t_{2,64} = -1.11$, $p = 0.271$, mean island $\pi_{orange} = 1.39 * 10^{-3}$, mean background $\pi_{orange} = 1.43 * 10^{-3}$, $t_{2,63} = -0.38$, $p = 0.702$). This suggests that genomic islands are likely arising from divergent selection between habitats and color morphs and not due to older sweeps predating the colonization of the Jordeweiher pond or due to other processes such as background selection (Cruickshank & Hahn 2014; Burri *et al.* 2015), which would instead reduce diversity in both groups at the same genomic regions.

We screened the gene content of genomic islands and found 847 overlapping genes, including 615 genes with orthologues in zebrafish (*Danio rerio*). We did not find enrichment for gene ontology categories among these 847 genes, but we identified a number of putative candidate genes with functions derived from zebrafish phenotypes (Howe *et al.* 2013) that are relevant to the observed phenotypic divergence among Jordeweiher males. The set of overlapping genes contained multiple genes with a role in visual perception, eye, retina and photoreceptor development, photoreceptor maintenance and recovery, genes controlling erythrocyte development responsible for red pigmentation, melanocyte development and iridophore development responsible for blue coloration . Those genes are distributed across multiple genomic islands found in this study, with many islands

containing candidate genes involved in both visual system and in pigmentation, which could be possible targets of divergent selection (e.g. island C.2a, C.3, H.11, C.20c, H.21a, Tab. S1).

The genomic islands overlap with 151 previously identified QTLs controlling morphology associated with feeding ecology, body shape and predator defense (Tab. S2). However, the overlap between QTLs and genomic islands is not significantly higher than expected if the islands were randomly distributed across the genome (permutation test, $p > 0.05$). Furthermore, none of these traits are differentiated among Jordeweiher males, while none of the few QTLs known to influence male nuptial coloration overlap with the observed genomic islands (Malek *et al.* 2012; Yong *et al.* 2015). Unlike the analysis of candidate genes, the analysis of QTL overlap thus did not reveal plausible functional connections between divergent phenotypes and the genetic basis of traits detected in other studies and populations.

Most of the genomic islands that we found overlap with genomic islands previously reported between other stickleback ecotypes or populations (Tab. S2): islands C.2a, C.2b, H.3, H.11, HC.12, C.20b/c and H.21a are also differentiated between parapatric lake and stream ecotypes in Canada, Germany and Switzerland (Kaeuffer *et al.* 2012; Feulner *et al.* 2015; Marques *et al.* 2016). Islands C.20a/b/c and H.21a were also divergent between multiple parapatric marine and freshwater stickleback populations from around the Northern Hemisphere (Jones *et al.* 2012b). Finally, islands C.3, H.11 and C.20a contain loci divergent among allopatric marine and freshwater populations (DeFaveri *et al.* 2011) and loci with evidence for balancing selection in marine and freshwater populations were detected in islands C.2b, H.7 and C.20c/d (Makinen *et al.* 2008b). With the exception of sympatric lake and stream stickleback from Lake Constance, which also differ in red / orange throat coloration (Marques *et al.* 2016), most of these other cases involved differentiation between allopatric or parapatric populations, for which despite the obvious habitat differences, differences in male nuptial coloration have not been reported.

Discussion

Our results reveal a rare case in stickleback of strong differentiation in a sexual signaling phenotype associated with habitat differences in sympatry, in the absence of differentiation in ecological and morphological traits related to resource acquisition and predator defense. The genomic landscape associated with this early divergence is characterized by multiple genomic islands of moderate differentiation located on several chromosomes. In many islands, diversity is reduced in one of the two morphs but not the other one, suggesting that selective sweeps occurred in both morphs but at different loci. We identified a number of possible targets of divergent selection in genomic islands of differentiation, genes that are involved in visual perception and eye morphogenesis.

Environmentally mediated divergent sexual selection as a likely driver of stable throat color polymorphism

Nuptial coloration is a product and target of sexual selection (Kodric-Brown & Brown 1984; Andersson 1994), with throat color being of particular importance in threespine stickleback (Bakker & Mundwiler 1994; Rush *et al.* 2003; Flamarique *et al.* 2013). Previous work on other stickleback populations showed that males with redder throats are preferred by females (Bakker & Mundwiler 1994), more dominant (Bakker & Milinski 1993), more successful in defending territory and offspring (Candolin & Tukiainen 2015) and in a better condition (Milinski & Bakker 1990; Boughman 2007). However, sexual selection on throat color has also been shown to be divergent between some populations and ecotypes, mainly depending on divergent visual environments (McKinnon & Rundle 2002). For example in stained waters on the North American Pacific coast, stickleback males have repeatedly acquired black throats (Semler 1971; Reimchen 1989; McKinnon 1995), a consequence of sexual selection maximizing male signal intensity or visibility to females against a background that is dominated by red light (Reimchen 1989; Boughman 2001; Lewandowski & Boughman 2008). Two studies (Malek *et al.* 2012; Yong *et al.* 2015) have identified a genetic basis for throat color controlling hue (red vs. black) and intensity (redness), confirming a certain degree of heritability for this sexual signal. Theory suggests that interactions between sexual selection and visually heterogeneous habitats lead to the evolution and maintenance of male color polymorphism under

415 many conditions (Chunco *et al.* 2007) and many examples exist for environment-associated
416 polymorphisms in male ornaments (Gray & McKinnon 2007) in guppies (Endler 1983; Cole & Endler
417 2015), cichlids (Seehausen & van Alphen 1999; Allender *et al.* 2003), killifish (Fuller 2002),
418 silversides (Gray *et al.* 2008) or Anolis lizards (Leal & Fleishman 2002).

419 The strong and stable association between male color morph and breeding habitat in the Jordeweiher
420 pond is likely driven by such environment-dependent divergent sexual selection. In another study
421 (Feller *et al.* 2016), we found a bimodal distribution of female preferences in this population
422 suggesting that the female population in this pond does not cause directional selection towards redder
423 throat coloration. Instead, females vary in their preferences for either red or orange males even when
424 tested in the same standard white light lab environment, suggesting some level of assortative mating
425 could be present in the pond (Feller *et al.* 2016). Red and orange nuptial coloration could therefore be
426 alternative strategies to maximize male attractiveness to females in different light regimes and against
427 different background colors, in response to divergent sexual selection imposed by females.
428 Divergence in nest types as an extended phenotype (Hunter 2009) may enhance male attractiveness in
429 the respective habitats (Kraak *et al.* 1999; Bolnick *et al.* 2015): nearshore males build shallower, less
430 conspicuous, hidden nests (Fig. 1b), while offshore males build open, crater-shaped nests at greater
431 depth (Fig. 1e). Both direct sexual selection against males in the ‘wrong’ habitat, male-male
432 competition and ‘habitat-matching’ (Edelaar *et al.* 2008), the active choice of the optimal breeding
433 habitat maximizing the impact of a male morph’s sexual signaling phenotype, may contribute to the
434 stability of this polymorphism.

435 Divergence in throat color could also be a product of the interaction between disruptive natural and
436 sexual selection between the two habitats: Predators may select for reduced conspicuousness and
437 camouflage, leading to different solutions in the two light regimes and background colors. This could
438 induce a trade-off between natural and sexual selection, which in turn may have caused offshore
439 males to compensate for being less red-throated by building more elaborate nests that might aid in
440 attracting females as shown elsewhere (Kraak *et al.* 1999). Also, predator composition and predation

pressure may vary between habitats. However, the predator fauna of the Jordeweiher is very impoverished compared with other stickleback habitats (Zeller *et al.* 2012), in particular piscivorous fish and birds – the latter putatively causing divergent predation pressure between habitats – are rare and divergent selection imposed by these predators may thus be irregular and overall not very strong. Furthermore, the magnitude of trait divergence was much larger in throat coloration than in typical predator defense or predator evasion (e.g. swimming performance) related traits, which was unexpected if predator composition or predator pressure differences between habitats would be a major source of divergent natural selection.

Little divergence in traits under direct natural selection

Traits commonly found to be under direct natural selection, such as predator defense, feeding ecology or swimming performance traits had not diverged between habitats or color morphs in the Jordeweiher. This is in strong contrast to most other cases of phenotypic divergence between stickleback populations occupying adjacent habitats, which commonly show strong morphological divergence in traits related to predator avoidance or feeding, rather than, or simultaneously with, divergence in sexually selected traits (McPhail 1994; McKinnon & Rundle 2002; Olafsdottir *et al.* 2006; Olafsdottir *et al.* 2007b, a; Cooper *et al.* 2011; Ravinet *et al.* 2013; Reimchen *et al.* 2013). Most well-studied stickleback ecotypes with divergence in mating signals show morphological divergence related to feeding and / or predator defense too, for example sympatric benthic and limnetic stickleback species in British Columbia (Schluter & McPhail 1992; McPhail 1994; Boughman *et al.* 2005), sympatric lake and stream stickleback from Lake Constance (Lucek *et al.* 2012; Moser *et al.* 2012) or allopatric stickleback from stained versus clear lakes on Haida Gwaii (Reimchen *et al.* 2013).

While a range of differences in habitats and selection regimes may explain phenotypic divergence between allopatric or parapatric populations, the major axis of phenotypic divergence in stickleback species coexisting in sympatry is benthic versus limnetic forms in freshwater lakes in British

Columbia (McPhail 1994). Although these forms are thought to have evolved from double-invasions of the lakes rather than from sympatric speciation (Taylor & McPhail 2000), ecological differentiation in sympatry is likely crucial to their coexistence and persistence (Schluter & McPhail 1992; Rundle *et al.* 2000; Vamosi & Schluter 2002; Arnegard *et al.* 2014). The weak divergence in ecological traits between habitats and color morphs in the Jordeweiher pond despite strong differentiation in mating traits may suggest that the fitness landscape for feeding related traits in this habitat does not cause strong disruptive selection, contrary to benthic and limnetic stickleback in Canadian lakes (Arnegard *et al.* 2014). The different predator community in the Jordeweiher, dominated by insects, adds to generating a selective landscape that is probably very different from those of the British Columbia lakes where trout as a predator is important (Vamosi & Schluter 2002; Rundle *et al.* 2003; Arnegard *et al.* 2014). Alternatively, it is possible that disruptive selection in Jordeweiher is dissipated by ecological dimorphism between the sexes instead of divergent ecological adaptation between color morphs (Bolnick & Lau 2008; Bolnick 2011; Cooper *et al.* 2011).

Genomic signature of early ecological speciation

While sympatric benthic and limnetic stickleback species from lakes in British Columbia show considerable reproductive isolation and genomic differentiation (McPhail 1994; Nagel & Schluter 1998; Rundle *et al.* 2000; Boughman 2001; Jones *et al.* 2012a), genome differentiation among Jordeweiher ecotypes is restricted to a few genomic islands of significantly elevated differentiation, similar to sympatric lake and stream ecotypes from Lake Constance (Marques *et al.* 2016). The evolution of Canadian benthic and limnetic stickleback species pairs involved an extensive phase of allopatry (Taylor & McPhail 2000) and genomic differentiation may reflect a mix of selective maintenance of adaptive differentiation, adaptive divergence in sympatry and random divergence due to historical contingency (Jones *et al.* 2012a). The Jordeweiher pond instead, as most of the surrounding populations in Central Switzerland, is inhabited by a population that arose from hybridization between at least two distinct stickleback lineages (Lucek *et al.* 2010; Roy *et al.* 2015) and the resulting genetic and phenotypic variation in the hybrid swarm may have facilitated incipient

492 speciation into color morphs divergently adapted to two adjacent habitat and therein ‘ecotypes’. The
493 fact that we find no elevated background differentiation in the genome with a number of genomic
494 islands is consistent with the hypothesis that the Jordeweiher pond was colonized only once by a
495 population from the hybrid zone rather than separately by each of the different lineages that gave rise
496 to the hybrid zone. It is therefore likely that genomic differentiation and stabilization among
497 Jordeweiher nearshore and offshore ecotypes is a product of very recent incipient speciation in
498 sympatry, possibly facilitated by the preceding formation of a hybrid swarm between divergent
499 lineages (Seehausen 2004, 2013).

500 Few well-documented examples of sympatric divergence exist (Bolnick & Fitzpatrick 2007) and
501 genomic differentiation has been studied in even fewer cases. Of the two cases that we know of,
502 *Rhagoletis* fruit flies and crater lake cichlids (Michel *et al.* 2010; Malinsky *et al.* 2015), many
503 genomic islands have been found, similar to the Jordeweiher stickleback. However, in *Rhagoletis* fruit
504 flies many of these islands were associated with inversions that diverged during periods of allopatry,
505 something that remains unknown in Jordeweiher stickleback and the crater lake cichlids. In contrast to
506 the Jordeweiher stickleback, weak but significant genome-wide background differentiation was
507 detectable in fruit flies diverging for 150 (Michel *et al.* 2010) and cichlids diverging for 10’000 years
508 (Malinsky *et al.* 2015). These differences in genomic background differentiation might be due to a
509 combination of variation in time since divergence started, levels of ongoing gene flow, and the
510 mechanisms of reproductive isolation, and varying population sizes and thus drift in different systems.

511 What are the traits coded in genomic islands under divergent selection? The presence of multiple
512 moderately differentiated islands in Jordeweiher stickleback suggest a rather complex genetic basis
513 for the traits under selection, controlled by genes on different chromosomes, and / or multifarious
514 selection on several traits leading to multiple differentiated genomic regions (Feder *et al.* 2012). The
515 presence of color perception and eye development genes may indicate that the perception of color and
516 therefore female preferences are targets of divergent sexual selection (Fig. 5). If female preference
517 was environment-dependent and genetically inherited, reproductive isolation between ecotypes could

be strengthened by sensory drive, the combination of habitat-specific transmission of male signal, perception adaptation in females and the matching of male signal and female perception (Boughman 2002). Sensory drive speciation is well-known from benthic and limnetic stickleback (Boughman 2001) and from *Pundamilia* cichlids (Seehausen *et al.* 2008) and may have led to sympatric speciation in the latter (Seehausen & van Alphen 1999; Seehausen *et al.* 2008). We do however not yet know whether sensory drive may operate as a mechanism of divergence among Jordeweiher sticklebacks. Measurement of the distribution of female mate preferences, excluding environmental effects, revealed a bimodal preference function among females (Feller *et al.* 2016), yet the strength of assortative mating under natural conditions remains unknown (Snowberg & Bolnick 2012). A better understanding of the environmental component of mate choice will be crucial to evaluate whether sensory drive may be operating and causing reproductive isolation in the Jordeweiher stickleback (Hendry *et al.* 2009).

Conclusions

We showed that two sympatric color morphs of threespine stickleback with a stable habitat association evolved in a 90 years old population, representing a very early stage of ecological speciation as defined by the emergence of divergence in multiple genomic regions in sympatry. The Jordeweiher pond stickleback are the youngest case of divergence between sympatric color morphs investigated at the genomic level, and thus the first snapshot of the genomic landscape associated with very early ecological speciation in which divergent sexual selection likely plays the lead role. Our results suggest that the genomic pattern associated with this process is characterized by multiple unlinked genomic islands against an undifferentiated genomic background. We encourage further search for other young sympatric color polymorphisms in stickleback, the genomic investigation of which would allow testing the generality of this pattern.

Acknowledgments

We would like to thank Matt McGee for advice regarding the measured suction feeding proxy, Carmela Doenz and students from the University of Bern practical in 2007 for assistance in the field, Salome Mwaiko for assistance in the lab, Denis Roy for the preparation and Richard Heemskerk from the Environmental Isotope Laboratory, University of Waterloo, for the analysis of stable isotope samples, as well as Aria Minder and Stefan Zoller from the Genetic Diversity Center (GDC), ETH Zurich/Eawag for bioinformatics support. This research was supported by Swiss National Science Foundation (SNF) grants PDFMP3_134657 to LE and OS.

References

Albert AY, Sawaya S, Vines TH, *et al.* (2008) The genetics of adaptive shape shift in stickleback: pleiotropy and effect size. *Evolution* **62**, 76-85.

Allender CJ, Seehausen O, Knight ME, Turner GF, Maclean N (2003) Divergent selection during speciation of Lake Malawi cichlid fishes inferred from parallel radiations in nuptial coloration. *Proceedings of the National Academy of Sciences of the United States of America* **100**, 14074-14079.

Andersson MB (1994) *Sexual selection* Princeton University Press, Princeton, N.J.

Andrews KR, Luikart G (2014) Recent novel approaches for population genomics data analysis. *Molecular Ecology* **23**, 1661-1667.

Arnegard ME, McGee MD, Matthews B, *et al.* (2014) Genetics of ecological divergence during speciation. *Nature* **511**, 307-311.

Baird NA, Etter PD, Atwood TS, *et al.* (2008) Rapid SNP discovery and genetic mapping using sequenced RAD markers. *PLoS One* **3**, e3376.

Bakker TCM, Milinski M (1993) The advantages of being red - sexual selection in the stickleback. *Marine Behaviour and Physiology* **23**, 287-300.

Bakker TCM, Mundwiler B (1994) Female mate choice and male red coloration in a natural 3-spined stickleback (*Gasterosteus aculeatus*) population. *Behavioral Ecology* **5**, 74-80.

Baxter SW, Davey JW, Johnston JS, *et al.* (2011) Linkage mapping and comparative genomics using next-generation RAD sequencing of a non-model organism. *PLoS One* **6**, e19315.

Benjamini Y, Hochberg Y (1995) Controlling the false discovery rate - a practical and powerful approach to multiple testing. *Journal of the Royal Statistical Society Series B-Methodological* **57**, 289-300.

Berner D, Moser D, Roesti M, Buescher H, Salzburger W (2014) Genetic architecture of skeletal evolution in European lake and stream stickleback. *Evolution* **68**, 1792-1805.

Bolnick DI (2011) Sympatric speciation in threespine stickleback: why not? *International Journal of Ecology* **2011**, 1-15.

Bolnick DI, Fitzpatrick BM (2007) Sympatric speciation: models and empirical evidence. *Annual Review of Ecology Evolution and Systematics* **38**, 459-487.

Bolnick DI, Lau OL (2008) Predictable patterns of disruptive selection in stickleback in postglacial lakes. *The American Naturalist* **172**, 1-11.

Bolnick DI, Shim KC, Brock CD (2015) Female stickleback prefer shallow males: Sexual selection on nest microhabitat. *Evolution* **69**, 1643-1653.

Boughman JW (2001) Divergent sexual selection enhances reproductive isolation in sticklebacks. *Nature* **411**, 944-948.

584 Boughman JW (2002) How sensory drive can promote speciation. *Trends in Ecology & Evolution* **17**,
585 571-577.
586 Boughman JW (2007) Condition-dependent expression of red colour differs between stickleback
587 species. *Journal of Evolutionary Biology* **20**, 1577-1590.
588 Boughman JW, Rundle HD, Schluter D (2005) Parallel evolution of sexual isolation in sticklebacks.
589 *Evolution* **59**, 361-373.
590 Burri R, Nater A, Kawakami T, *et al.* (2015) Linked selection and recombination rate variation drive
591 the evolution of the genomic landscape of differentiation across the speciation continuum of
592 Ficedula flycatchers. *Genome Research* **25**, 1656-1665.
593 Candolin U, Tukiainen I (2015) The sexual selection paradigm: have we overlooked other
594 mechanisms in the evolution of male ornaments? *Proceedings of the Royal Society B-*
595 *Biological Sciences* **282**, 20151987.
596 Catchen JM, Amores A, Hohenlohe P, Cresko W, Postlethwait JH (2011) Stacks: building and
597 genotyping loci de novo from short-read sequences. *G3* **1**, 171-182.
598 Chan YF, Marks ME, Jones FC, *et al.* (2010) Adaptive evolution of pelvic reduction in sticklebacks
599 by recurrent deletion of a Pitx1 enhancer. *Science* **327**, 302-305.
600 Chan YF, Villarreal G, Marks M, *et al.* (2009) From trait to base pairs: Parallel evolution of pelvic
601 reduction in three-spined sticklebacks occurs by repeated deletion of a tissue-specific pelvic
602 enhancer at Pitx1. *Mechanisms of Development* **126**, S14-S15.
603 Chunco AJ, McKinnon JS, Servedio MR (2007) Microhabitat variation and sexual selection can
604 maintain male color polymorphisms. *Evolution* **61**, 2504-2515.
605 Cleves PA, Ellis NA, Jimenez MT, *et al.* (2014) Evolved tooth gain in sticklebacks is associated with
606 a cis-regulatory allele of Bmp6. *Proceedings of the National Academy of Sciences of the*
607 *United States of America* **111**, 13912-13917.
608 Cole GL, Endler JA (2015) Variable environmental effects on a multicomponent sexually selected
609 trait. *The American Naturalist* **185**, 452-468.
610 Colosimo PF, Hosemann KE, Balabhadra S, *et al.* (2005) Widespread parallel evolution in
611 sticklebacks by repeated fixation of Ectodysplasin alleles. *Science* **307**, 1928-1933.
612 Colosimo PF, Peichel CL, Nereng K, *et al.* (2004) The genetic architecture of parallel armor plate
613 reduction in threespine sticklebacks. *PLoS Biology* **2**, E109.
614 Conte GL, Arnegard ME, Best J, *et al.* (2015) Extent of QTL Reuse During Repeated Phenotypic
615 Divergence of Sympatric Threespine Stickleback. *Genetics* **201**, 1189-1200.
616 Cooper IA, Gilman RT, Boughman JW (2011) Sexual dimorphism and speciation on two ecological
617 coins: patterns from nature and theoretical predictions. *Evolution* **65**, 2553-2571.
618 Coyle SM, Huntingford FA, Peichel CL (2007) Parallel evolution of Pitx1 underlies pelvic reduction
619 in Scottish threespine stickleback (*Gasterosteus aculeatus*). *Journal of Heredity* **98**, 581-586.
620 Coyne JA, Orr HA (2004) *Speciation* Sinauer Assoc, Sunderland, MA.
621 Cresko WA, Amores A, Wilson C, *et al.* (2004) Parallel genetic basis for repeated evolution of armor
622 loss in Alaskan threespine stickleback populations. *Proceedings of the National Academy of*
623 *Sciences of the United States of America* **101**, 6050-6055.
624 Cruickshank TE, Hahn MW (2014) Reanalysis suggests that genomic islands of speciation are due to
625 reduced diversity, not reduced gene flow. *Molecular Ecology* **23**, 3133-3157.
626 Danecek P, Auton A, Abecasis G, *et al.* (2011) The variant call format and VCFtools. *Bioinformatics*
627 **27**, 2156-2158.
628 Davey JW, Cezard T, Fuentes-Utrilla P, *et al.* (2013) Special features of RAD sequencing data:
629 implications for genotyping. *Molecular Ecology* **22**, 3151-3164.
630 Davey JW, Hohenlohe PA, Etter PD, *et al.* (2011) Genome-wide genetic marker discovery and
631 genotyping using next-generation sequencing. *Nature Reviews Genetics* **12**, 499-510.
632 Deagle BE, Jones FC, Chan YF, *et al.* (2012) Population genomics of parallel phenotypic evolution in
633 stickleback across stream-lake ecological transitions. *Proceedings of the Royal Society B-*
634 *Biological Sciences* **279**, 1277-1286.

DeFaveri J, Shikano T, Shimada Y, Goto A, Merila J (2011) Global analysis of genes involved in freshwater adaptation in threespine sticklebacks (*Gasterosteus aculeatus*). *Evolution* **65**, 1800-1807.

Edelaar P, Siepielski AM, Clobert J (2008) Matching habitat choice causes directed gene flow: a neglected dimension in evolution and ecology. *Evolution* **62**, 2462-2472.

Ellis NA, Glazer AM, Donde NN, *et al.* (2015) Distinct developmental genetic mechanisms underlie convergently evolved tooth gain in sticklebacks. *Development* **142**, 2442-2451.

Endler JA (1983) Natural and sexual selection on color patterns in Poeciliid fishes. *Environmental Biology of Fishes* **9**, 173-190.

Erickson PA, Cleves PA, Ellis NA, *et al.* (2015) A 190 base pair, TGF-beta responsive tooth and fin enhancer is required for stickleback Bmp6 expression. *Developmental Biology* **401**, 310-323.

Erickson PA, Glazer AM, Cleves PA, Smith AS, Miller CT (2014) Two developmentally temporal quantitative trait loci underlie convergent evolution of increased branchial bone length in sticklebacks. *Proceedings of the Royal Society B-Biological Sciences* **281**, 20140822.

Erickson PA, Glazer AM, Killingbeck EE, *et al.* (2016) Partially repeatable genetic basis of benthic adaptation in threespine sticklebacks. *Evolution* **70**, 887-902.

Excoffier L, Lischer HE (2010) Arlequin suite ver 3.5: a new series of programs to perform population genetics analyses under Linux and Windows. *Molecular Ecology Resources* **10**, 564-567.

Feder JL, Egan SP, Nosil P (2012) The genomics of speciation-with-gene-flow. *Trends in Genetics* **28**, 342-350.

Feller AF, Seehausen O, Lucek K, Marques DA (2016) Habitat choice and female preference in a polymorphic stickleback population. *Evolutionary Ecology Research* **17**, 419–435.

Feulner PG, Chain FJ, Panchal M, *et al.* (2015) Genomics of divergence along a continuum of parapatric population differentiation. *PLoS Genetics* **11**, e1004966.

Flamarique IN, Bergstrom C, Cheng CL, Reimchen TE (2013) Role of the iridescent eye in stickleback female mate choice. *Journal of Experimental Biology* **216**, 2806-2812.

Fraley C, Raftery AE (2002) Model-based clustering, discriminant analysis, and density estimation. *Journal of the American Statistical Association* **97**, 611-631.

Franceschini A, Szklarczyk D, Frankild S, *et al.* (2013) STRING v9.1: protein-protein interaction networks, with increased coverage and integration. *Nucleic Acids Res* **41**, D808-815.

Fuller RC (2002) Lighting environment predicts the relative abundance of male colour morphs in bluefin killifish (*Lucania goodei*) populations. *Proceedings of the Royal Society B-Biological Sciences* **269**, 1457-1465.

Glazer AM, Cleves PA, Erickson PA, Lam AY, Miller CT (2014) Parallel developmental genetic features underlie stickleback gill raker evolution. *Evodevo* **5**, 19.

Glazer AM, Killingbeck EE, Mitros T, Rokhsar DS, Miller CT (2015) Genome assembly improvement and mapping convergently evolved skeletal traits in sticklebacks with genotyping-by-sequencing. *G3* **5**, 1463-1472.

Gray SM, Dill LM, Tantu FY, *et al.* (2008) Environment-contingent sexual selection in a colour polymorphic fish. *Proceedings of the Royal Society B-Biological Sciences* **275**, 1785-1791.

Gray SM, McKinnon JS (2007) Linking color polymorphism maintenance and speciation. *Trends in Ecology & Evolution* **22**, 71-79.

Greenwood AK, Ardekani R, McCann SR, *et al.* (2015) Genetic mapping of natural variation in schooling tendency in the threespine stickleback. *G3* **5**, 761-769.

Greenwood AK, Cech JN, Peichel CL (2012) Molecular and developmental contributions to divergent pigment patterns in marine and freshwater sticklebacks. *Evolution & Development* **14**, 351-362.

Greenwood AK, Jones FC, Chan YF, *et al.* (2011) The genetic basis of divergent pigment patterns in juvenile threespine sticklebacks. *Heredity* **107**, 155-166.

Greenwood AK, Wark AR, Yoshida K, Peichel CL (2013) Genetic and neural modularity underlie the evolution of schooling behavior in threespine sticklebacks. *Current Biology* **23**, 1884-1888.

687 Guo B, DeFaveri J, Sotelo G, Nair A, Merila J (2015) Population genomic evidence for adaptive
688 differentiation in Baltic Sea three-spined sticklebacks. *BMC Biology* **13**, 19.
689 Guo SW, Thompson EA (1992) Performing the exact test of Hardy-Weinberg proportion for multiple
690 alleles. *Biometrics* **48**, 361-372.
691 Hendry AP, Bolnick DI, Berner D, Peichel CL (2009) Along the speciation continuum in
692 sticklebacks. *Journal of Fish Biology* **75**, 2000-2036.
693 Hofer T, Foll M, Excoffier L (2012) Evolutionary forces shaping genomic islands of population
694 differentiation in humans. *BMC Genomics* **13**, 107.
695 Hohenlohe PA, Bassham S, Etter PD, *et al.* (2010) Population genomics of parallel adaptation in
696 threespine stickleback using sequenced RAD tags. *PLoS Genetics* **6**, e1000862.
697 Howe DG, Bradford YM, Conlin T, *et al.* (2013) ZFIN, the zebrafish model organism database:
698 increased support for mutants and transgenics. *Nucleic Acids Res* **41**, D854-860.
699 Hunter P (2009) Extended phenotype redux. How far can the reach of genes extend in manipulating
700 the environment of an organism? *EMBO reports* **10**, 212-215.
701 Jones FC, Chan YF, Schmutz J, *et al.* (2012a) A genome-wide SNP genotyping array reveals patterns
702 of global and repeated species-pair divergence in sticklebacks. *Current Biology* **22**, 83-90.
703 Jones FC, Grabherr MG, Chan YF, *et al.* (2012b) The genomic basis of adaptive evolution in
704 threespine sticklebacks. *Nature* **484**, 55-61.
705 Kaeuffer R, Peichel CL, Bolnick DI, Hendry AP (2012) Parallel and nonparallel aspects of ecological,
706 phenotypic, and genetic divergence across replicate population pairs of lake and stream
707 stickleback. *Evolution* **66**, 402-418.
708 Kimmel CB, Ullmann B, Walker C, *et al.* (2005) Evolution and development of facial bone
709 morphology in threespine sticklebacks. *Proceedings of the National Academy of Sciences of*
710 *the United States of America* **102**, 5791-5796.
711 Kitano J, Lema SC, Luckenbach JA, *et al.* (2010) Adaptive divergence in the thyroid hormone
712 signaling pathway in the stickleback radiation. *Current Biology* **20**, 2124-2130.
713 Kitano J, Ross JA, Mori S, *et al.* (2009) A role for a neo-sex chromosome in stickleback speciation.
714 *Nature* **461**, 1079-1083.
715 Kitano J, Yoshida K, Suzuki Y (2013) RNA sequencing reveals small RNAs differentially expressed
716 between incipient Japanese threespine sticklebacks. *BMC Genomics* **14**, 214.
717 Klingenberg CP (2011) MorphoJ: an integrated software package for geometric morphometrics.
718 *Molecular Ecology Resources* **11**, 353-357.
719 Kodric-Brown A, Brown JH (1984) Truth in advertising - the kinds of traits favored by sexual
720 selection. *The American Naturalist* **124**, 309-323.
721 Kraak SBM, Bakker TCM, Mundwiler B (1999) Sexual selection in sticklebacks in the field:
722 correlates of reproductive, mating, and paternal success. *Behavioral Ecology* **10**, 696-706.
723 Langmead B, Salzberg SL (2012) Fast gapped-read alignment with Bowtie 2. *Nature Methods* **9**, 357-
724 359.
725 Leal M, Fleishman LJ (2002) Evidence for habitat partitioning based on adaptation to environmental
726 light in a pair of sympatric lizard species. *Proceedings of the Royal Society B-Biological*
727 *Sciences* **269**, 351-359.
728 Lewandowski E, Boughman JW (2008) Effects of genetics and light environment on colour
729 expression in threespine sticklebacks. *Biological Journal of the Linnean Society* **94**, 663-673.
730 Lischer HE, Excoffier L (2012) PGDSpider: an automated data conversion tool for connecting
731 population genetics and genomics programs. *Bioinformatics* **28**, 298-299.
732 Liu J, Shikano T, Leinonen T, *et al.* (2014) Identification of major and minor QTL for ecologically
733 important morphological traits in three-spined sticklebacks (*Gasterosteus aculeatus*). *G3* **4**,
734 595-604.
735 Lucek K, Roy D, Bezault E, Sivasundar A, Seehausen O (2010) Hybridization between distant
736 lineages increases adaptive variation during a biological invasion: stickleback in Switzerland.
737 *Molecular Ecology* **19**, 3995-4011.

738 Lucek K, Sivasundar A, Roy D, Seehausen O (2013) Repeated and predictable patterns of ecotypic
739 differentiation during a biological invasion: lake-stream divergence in parapatric Swiss
740 stickleback. *Journal of Evolutionary Biology* **26**, 2691-2709.
741 Lucek K, Sivasundar A, Seehausen O (2012) Evidence of adaptive evolutionary divergence during
742 biological invasion. *PLoS One* **7**, e49377.
743 Maan ME, Seehausen O (2011) Ecology, sexual selection and speciation. *Ecology Letters* **14**, 591-
744 602.
745 Makinen HS, Cano JM, Merila J (2008a) Identifying footprints of directional and balancing selection
746 in marine and freshwater three-spined stickleback (*Gasterosteus aculeatus*) populations.
747 *Molecular Ecology* **17**, 3565-3582.
748 Makinen HS, Shikano T, Cano JM, Merila J (2008b) Hitchhiking mapping reveals a candidate
749 genomic region for natural selection in three-spined stickleback chromosome VIII. *Genetics*
750 **178**, 453-465.
751 Malek TB, Boughman JW, Dworkin I, Peichel CL (2012) Admixture mapping of male nuptial colour
752 and body shape in a recently formed hybrid population of threespine stickleback. *Molecular*
753 *Ecology* **21**, 5265-5279.
754 Malinsky M, Challis RJ, Tyers AM, *et al.* (2015) Genomic islands of speciation separate cichlid
755 ecomorphs in an East African crater lake. *Science* **350**, 1493-1498.
756 Marques DA, Lucek K, Meier JI, *et al.* (2016) Genomics of rapid incipient speciation in sympatric
757 threespine stickleback. *PLoS Genetics* **12**, e1005887.
758 Martin SH, Dasmahapatra KK, Nadeau NJ, *et al.* (2013) Genome-wide evidence for speciation with
759 gene flow in *Heliconius* butterflies. *Genome Research* **23**, 1817-1828.
760 McKenna A, Hanna M, Banks E, *et al.* (2010) The Genome Analysis Toolkit: a MapReduce
761 framework for analyzing next-generation DNA sequencing data. *Genome Research* **20**, 1297-
762 1303.
763 McKinnon JS (1995) Video mate preferences of female three-spined sticklebacks from populations
764 with divergent male coloration. *Animal Behaviour* **50**, 1645-1655.
765 McKinnon JS, Rundle HD (2002) Speciation in nature: the threespine stickleback model systems.
766 *Trends in Ecology & Evolution* **17**, 480-488.
767 McPhail J (1994) Speciation and the evolution of reproductive isolation in the sticklebacks
768 (*Gasterosteus*) of south-western British Columbia. In: *The evolutionary biology of the*
769 *threespine stickleback* (eds. Bell MA, Foster SA), pp. 399-437. Oxford Science Publications.
770 Michel AP, Sim S, Powell TH, *et al.* (2010) Widespread genomic divergence during sympatric
771 speciation. *Proceedings of the National Academy of Sciences of the United States of America*
772 **107**, 9724-9729.
773 Milinski M, Bakker TCM (1990) Female sticklebacks use male coloration in mate choice and hence
774 avoid parasitized males. *Nature* **344**, 330-333.
775 Miller CT, Beleza S, Pollen AA, *et al.* (2007) cis-Regulatory changes in Kit ligand expression and
776 parallel evolution of pigmentation in sticklebacks and humans. *Cell* **131**, 1179-1189.
777 Miller CT, Glazer AM, Summers BR, *et al.* (2014) Modular skeletal evolution in sticklebacks is
778 controlled by additive and clustered quantitative trait Loci. *Genetics* **197**, 405-420.
779 Moser D, Roesti M, Berner D (2012) Repeated lake-stream divergence in stickleback life history
780 within a Central European lake basin. *PLoS One* **7**, e50620.
781 Nadeau NJ, Whibley A, Jones RT, *et al.* (2012) Genomic islands of divergence in hybridizing
782 *Heliconius* butterflies identified by large-scale targeted sequencing. *Philosophical*
783 *Transactions of the Royal Society B-Biological Sciences* **367**, 343-353.
784 Nagel L, Schluter D (1998) Body size, natural selection, and speciation in sticklebacks. *Evolution* **52**,
785 209-218.
786 Nosil P (2012) *Ecological speciation* Oxford University Press, Oxford.
787 Nosil P, Egan SP, Funk DJ (2008) Heterogeneous genomic differentiation between walking-stick
788 ecotypes: "isolation by adaptation" and multiple roles for divergent selection. *Evolution* **62**,
789 316-336.

Olafsdottir GA, Ritchie MG, Snorrason SS (2006) Positive assortative mating between recently described sympatric morphs of Icelandic sticklebacks. *Biol Lett* **2**, 250-252.
Olafsdottir GA, Snorrason SS, Ritchie MG (2007a) Morphological and genetic divergence of intralacustrine stickleback morphs in Iceland: a case for selective differentiation? *Journal of Evolutionary Biology* **20**, 603-616.
Olafsdottir GA, Snorrason SS, Ritchie MG (2007b) Postglacial intra-lacustrine divergence of Icelandic threespine stickleback morphs in three neovolcanic lakes. *Journal of Evolutionary Biology* **20**, 1870-1881.
Peichel CL, Nereng KS, Ohgi KA, *et al.* (2001) The genetic architecture of divergence between threespine stickleback species. *Nature* **414**, 901-905.
Preucil F (1953) Color hue and ink transfer - their relation to perfect reproduction. *Technical Association of the Graphic Arts Proceedings*, 102-110.
Puritz JB, Matz MV, Toonen RJ, *et al.* (2014) Demystifying the RAD fad. *Molecular Ecology* **23**, 5937-5942.
QGIS Development Team (2015) *QGIS Geographic Information System. Open source geospatial foundation project.* http://qgis.osgeo.org
R Development Core Team (2015) *R: A language and environment for statistical computing.* R Foundation for Statistical Computing, Vienna, Austria. http://www.R-project.org/
Ravinet M, Prodohl PA, Harrod C (2013) Parallel and nonparallel ecological, morphological and genetic divergence in lake-stream stickleback from a single catchment. *Journal of Evolutionary Biology* **26**, 186-204.
Reimchen TE (1989) Loss of nuptial dolor in threespine sticklebacks (*Gasterosteus aculeatus*). *Evolution* **43**, 450-460.
Reimchen TE, Bergstrom C, Nosil P (2013) Natural selection and the adaptive radiation of Haida Gwaii stickleback. *Evolutionary Ecology Research* **15**, 241-269.
Renaut S, Grassa CJ, Yeaman S, *et al.* (2013) Genomic islands of divergence are not affected by geography of speciation in sunflowers. *Nature Communications* **4**, 1827.
Rice AM, Rudh A, Ellegren H, Qvarnstrom A (2011) A guide to the genomics of ecological speciation in natural animal populations. *Ecology Letters* **14**, 9-18.
Roesti M, Kueng B, Moser D, Berner D (2015) The genomics of ecological vicariance in threespine stickleback fish. *Nature Communications* **6**, 8767.
Rogers SM, Tamkee P, Summers B, *et al.* (2012) Genetic signature of adaptive peak shift in threespine stickleback. *Evolution* **66**, 2439-2450.
Rohlf FJ (2015) The tps series of software. *Hystrix-Italian Journal of Mammalogy* **26**, 9-12.
Roy D, Lucek K, Walter RP, Seehausen O (2015) Hybrid 'superswarm' leads to rapid divergence and establishment of populations during a biological invasion. *Molecular Ecology* **24**, 5394-5411.
Rundle HD, Nagel L, Wenrick Boughman J, Schluter D (2000) Natural selection and parallel speciation in sympatric sticklebacks. *Science* **287**, 306-308.
Rundle HD, Nosil P (2005) Ecological speciation. *Ecology Letters* **8**, 336-352.
Rundle HD, Vamosi SM, Schluter D (2003) Experimental test of predation's effect on divergent selection during character displacement in sticklebacks. *Proceedings of the National Academy of Sciences of the United States of America* **100**, 14943-14948.
Rush VN, McKinnon JS, Abney MA, Sargent RC (2003) Reflectance spectra from free-swimming sticklebacks (*Gasterosteus*): social context and eye-jaw contrast. *Behaviour* **140**, 1003-1019.
Sanger F, Air GM, Barrell BG, *et al.* (1977) Nucleotide sequence of bacteriophage phi X174 DNA. *Nature* **265**, 687-695.
Schluter D, McPhail JD (1992) Ecological character displacement and speciation in sticklebacks. *The American Naturalist* **140**, 85-108.
Schneider CA, Rasband WS, Eliceiri KW (2012) NIH Image to ImageJ: 25 years of image analysis. *Nature Methods* **9**, 671-675.
Seehausen O (2004) Hybridization and adaptive radiation. *Trends in Ecology & Evolution* **19**, 198-207.

Seehausen O (2013) Conditions when hybridization might predispose populations for adaptive radiation. *Journal of Evolutionary Biology* **26**, 279-281.
Seehausen O, Butlin RK, Keller I, *et al.* (2014) Genomics and the origin of species. *Nature Reviews Genetics* **15**, 176-192.
Seehausen O, Terai Y, Magalhaes IS, *et al.* (2008) Speciation through sensory drive in cichlid fish. *Nature* **455**, 620-626.
Seehausen O, van Alphen JM (1999) Can sympatric speciation by disruptive sexual selection explain rapid evolution of cichlid diversity in Lake Victoria? *Ecology Letters* **2**, 262-271.
Semler DE (1971) Some aspects of adaptation in a polymorphism for breeding colours in threespine stickleback (*Gasterosteus aculeatus*). *Journal of Zoology* **165**, 291-&.
Shapiro MD, Marks ME, Peichel CL, *et al.* (2004) Genetic and developmental basis of evolutionary pelvic reduction in threespine sticklebacks. *Nature* **428**, 717-723.
Shimada Y, Shikano T, Merila J (2011) A high incidence of selection on physiologically important genes in the three-spined stickleback, *Gasterosteus aculeatus*. *Molecular Biology and Evolution* **28**, 181-193.
Snowberg LK, Bolnick DI (2012) Partitioning the effects of spatial isolation, nest habitat, and individual diet in causing assortative mating within a population of threespine stickleback. *Evolution* **66**, 3582-3594.
Soria-Carrasco V, Gompert Z, Comeault AA, *et al.* (2014) Stick insect genomes reveal natural selection's role in parallel speciation. *Science* **344**, 738-742.
Stengel JR, Lutz R (1901) Kirchlindach. In: *Topographischer Atlas der Schweiz*. Schweizerisches Eidgenössisches Staatsbureau, H. Müllhaupt & Sohn, Bern.
Sun WG, Cai TT (2009) Large-scale multiple testing under dependence. *Journal of the Royal Statistical Society Series B-Statistical Methodology* **71**, 393-424.
swisstopo (2015) *Luftbild 19310310030627, May 11, 1931*. http://map.lubis.admin.ch/
Taylor EB, McPhail JD (2000) Historical contingency and ecological determinism interact to prime speciation in sticklebacks, *Gasterosteus*. *Proceedings of the Royal Society B-Biological Sciences* **267**, 2375-2384.
Terekhanova NV, Logacheva MD, Penin AA, *et al.* (2014) Fast evolution from precast bricks: genomics of young freshwater populations of threespine stickleback *Gasterosteus aculeatus*. *PLoS Genetics* **10**, e1004696.
Vamosi SM, Schluter D (2002) Impacts of trout predation on fitness of sympatric sticklebacks and their hybrids. *Proceedings of the Royal Society B-Biological Sciences* **269**, 923-930.
Vines TH, Schluter D (2006) Strong assortative mating between allopatric sticklebacks as a by-product of adaptation to different environments. *Proceedings of the Royal Society B-Biological Sciences* **273**, 911-916.
Wark AR, Mills MG, Dang LH, *et al.* (2012) Genetic architecture of variation in the lateral line sensory system of threespine sticklebacks. *G3* **2**, 1047-1056.
Wei Z, Sun W, Wang K, Hakonarson H (2009) Multiple testing in genome-wide association studies via hidden Markov models. *Bioinformatics* **25**, 2802-2808.
Wu CI (2001) The genic view of the process of speciation. *Journal of Evolutionary Biology* **14**, 851-865.
Yong L, Peichel CL, McKinnon JS (2015) Genetic architecture of conspicuous red ornaments in female threespine stickleback. *G3 (Bethesda)* **6**, 579-588.
Yoshida K, Makino T, Yamaguchi K, *et al.* (2014) Sex chromosome turnover contributes to genomic divergence between incipient stickleback species. *PLoS Genetics* **10**, e1004223.
Zeller M, Lucek K, Haesler MP, Seehausen O, Sivasundar A (2012) Signals of predation-induced directional and disruptive selection in the threespine stickleback. *Evolutionary Ecology Research* **14**, 193-205.

892 **Data accessibility**

893 FASTQ-files with de-multiplexed and base-quality score recalibrated reads have been deposited in the
894 short read archive (www.ncbi.nlm.nih.gov/sra) under accession SRP079408, ecological and
895 morphological data on Dryad (doi: http://dx.doi.org/10.5061/dryad.js08q).

896 **Author contributions**

897 DAM, OS, KL, MPH and AFF collected data in the field, DAM, KL and AFF analyzed the data with
898 assistance from LE and OS, DAM wrote the paper, OS, KL, LE, JIM and CEW revised the paper.

899

Tables

Table 1. Linear mixed effects model results for morphological and ecological traits, with summary statistics given for the predictors habitat and color, respectively. Significant traits / models after correction for multiple testing are highlighted in bold.

Trait	Abbr.	Habitat			Color		
		β_{trait}	$t_{2,55}$*	p-value	β_{trait}	$t_{2,55}$*	p-value
standard length	SL	1.785	2.221	0.030	**2.389**	**2.938**	**0.005**
head length	HL	0.251	2.134	0.037	0.192	1.554	0.126
snout length	SnL	0.097	1.521	0.134	0.048	0.742	0.461
eye diameter	ED	0.078	1.576	0.121	0.039	0.771	0.444
upper jaw length	UJL	0.148	2.404	0.020	0.124	1.924	0.060
suction index proxy	SucP	0.307	2.033	0.047	0.295	1.870	0.067
first spine length	FSL	0.034	0.370	0.713	0.004	0.049	0.961
second spine length	SSL	0.158	1.958	0.055	0.220	2.773	0.008
pelvic spine length	PSL	0.054	0.510	0.612	0.059	0.545	0.588
body depth 1	BD1	0.298	2.386	0.021	**0.371**	**2.930**	**0.005**
body depth 2	BD2	0.337	2.783	0.007	**0.381**	**3.064**	**0.003**
total length pelvic fin	TLP	0.070	0.689	0.494	0.020	0.185	0.854
basal length pelvic fin	BLP	0.018	0.403	0.689	0.012	0.261	0.795
basal length dorsal fin	BLD	**0.282**	**2.973**	**0.004**	**0.363**	**3.838**	**<0.001**
basal length anal fin	BLA	0.212	1.820	0.074	0.016	0.129	0.898
caudal peduncle length	CPL	0.077	0.652	0.517	0.018	0.153	0.879
caudal peduncle depth	CPD	0.027	0.879	0.383	0.011	0.348	0.729
all linear traits PC1	-	**0.665**	**2.952**	**0.005**	**0.723**	**3.118**	**0.003**
feeding traits PC1	-	0.436	2.377	0.021	0.382	1.981	0.053
defense traits PC1	-	0.099	0.747	0.458	0.148	1.127	0.265
swimming traits PC1	-	0.495	2.674	0.010	**0.621**	**3.330**	**0.002**
throat color	-	**10.936**	**6.078**	**<0.001**	–	–	–
head + body shape PC2	-	0.003	0.536	0.594	0.008	1.418	0.162
body shape PC1	-	0.018	2.708	0.009	**0.022**	**3.365**	**0.001**
head shape PC1	-	0.000	0.054	0.957	0.007	0.931	0.356
δ^{13}carbon	δ^{13}C	1.948	1.650	0.127	1.397	1.055	0.314
δ^{15}nitrogen	δ^{15}N	0.764	1.570	0.145	0.443	0.803	0.439
proportion of planktonic prey	PPP	0.074	0.449	0.659	0.185	1.100	0.288

*$t_{2,11}$ for δ^{13}C / δ^{15}N and $t_{2,16}$ for PPP.

906 Table 2. Position and size of genomic islands of differentiation among male color morphs (C) and
907 males breeding in different habitats (H), as well as islands found in both comparisons (HC).

Island name	Chromosome	Start*	End*	Length	No. of SNPs
H.3	chrIII	10,195,189	11,013,253	818,065	18
H.7	chrVII	29,369,008	29,580,946	211,939	12
H.11	chrXI	15,670,181	16,461,683	791,503	21
HC.12	chrXII	5,238,787	5,776,374	537,588	19
HC.14	chrXIV	2,990,195	3,400,864	410,670	18
H.16	chrXVI	17,953,430	18,437,334	483,905	26
HC.18	chrXVIII	12,115,653	12,700,449	584,797	21
H.21a	chrXXI	3,569,648	6,950,491	3,380,844	18
H.21b	chrXXI	12,637,551	12,876,396	238,846	10
C.2a	chrII	4,559,861	6,181,686	1,621,825	46
C.2b	chrII	23,256,982	23,687,419	430,437	11
C.3	chrIII	9,275,841	9,275,999	158	6
C.10	chrX	6,932,366	7,012,361	79,995	7
HC.12	chrXII	5,387,615	5,706,897	319,282	14
HC.14	chrXIV	2,377,579	3,131,078	753,499	33
C.17	chrXVII	4,900,840	5,033,507	132,667	6
HC.18	chrXVIII	11,702,348	12,700,449	998,101	28
C.18a	chrXVIII	13,194,103	13,453,530	259,427	15
C.18b	chrXVIII	13,483,346	14,067,086	583,740	10
C.20a	chrXX	363,978	956,341	592,363	21
C.20b	chrXX	4,850,891	6,519,852	1,668,961	44
C.20c	chrXX	6,619,982	8,049,063	1,429,081	21
C.20d	chrXX	9,363,001	9,607,463	244,462	6

908 *Coordinates from the re-assembly by Glazer *et al.* (2015).

909

Figures

Fig. 1. Threespine stickleback breed in two divergent habitats, ‘offshore’ (a-c) and ‘nearshore’ (d-f), in the Jordeweiher pond near Bern, Switzerland. While offshore habitat (a) consists of an open, flat, muddy floor, with direct sunlight and greater depth down to 3 m, nearshore habitat (d) is a steep clay bank below overhanging trees producing a more heterogeneous and dynamic light mosaic and a more complex habitat with branches, tree roots and leaves. Stickleback males breeding in offshore habitat (c) have an orange throat and pale body color and build large, deep crater nests (b), while nearshore breeding males (f) have a red throat and a darker body with more dark pigments and build concealed nests (e).

Fig. 2. Bimodal distribution of throat color and phenotype-environment association in Jordeweiher threespine stickleback. a) Throat color distribution and cluster analysis assignment of each male (colored vertical bars) to the two supported ‘red’ and ‘orange’ clusters. b) The phenotype-environment association is significant using both continuous variables (hue, depth, males from 2013 and 2015 only, see text for statistics) as well as c) discrete habitat categories (blue dots: offshore, black dots: nearshore), the latter demonstrating temporal stability of the throat color vs breeding habitat association for at least 9 years. Symbols show the intensity of nuptial coloration: Males sampled in 2012 showed more faded nuptial coloration, likely due to the early sampling date in the year and the capture using minnow traps.

930 Fig. 3. Distribution of nests in the Jordeweiher across breeding habitats. Steep nearshore habitat,
931 where predominantly red-throated males build their nests, is mostly found at the Eastern side of the
932 pond. The flat offshore habitat covers most of the pond bottom, where mostly orange-throated males
933 breed.

934

935 Fig. 4. Phenotypic (P_{ST}) and ecological (E_{ST}) differentiation between stickleback males grouped by
936 breeding habitat and color morph. Habitat differentiation is only significant for throat color, a sexual
937 signal, while no differentiation is present in morphological traits associated with feeding, defense and
938 swimming performance. Filled and empty symbols indicate groups with higher absolute or residual
939 values for raw and size-corrected traits respectively. See Table 1 for trait abbreviations. Whiskers
940 indicate 95% confidence intervals from 1,000 bootstrap permutations for P_{ST} and E_{ST} (feeding
941 ecology) estimates. Asterisks indicate significant P_{ST} estimates (***: $p<0.001$).

942

Fig. 5. Distribution of pairwise differentiation (F_{ST}) and differences in nucleotide diversity ($\Delta\pi$) across the genome between Jordeweiher males grouped by color morph and breeding habitat. Genomic islands, regions with an accumulation of increased differentiation loci, are named with italic letters (see Tab. 1) and highlighted with grey vertical bars, black colored SNPs (F_{ST}) and black colored overlapping windows ($\Delta\pi$) respectively. Three genomic islands on chrXII, chrXIV and XVIII are found both among males grouped by color morph and habitat (blue vertical bars). While on average, stickleback males are not differentiated across most of their genome, genomic islands harbor moderately divergent SNPs, ranging up to $F_{ST} = 0.46$ (color morphs) and $F_{ST} = 0.48$ (habitat), respectively.

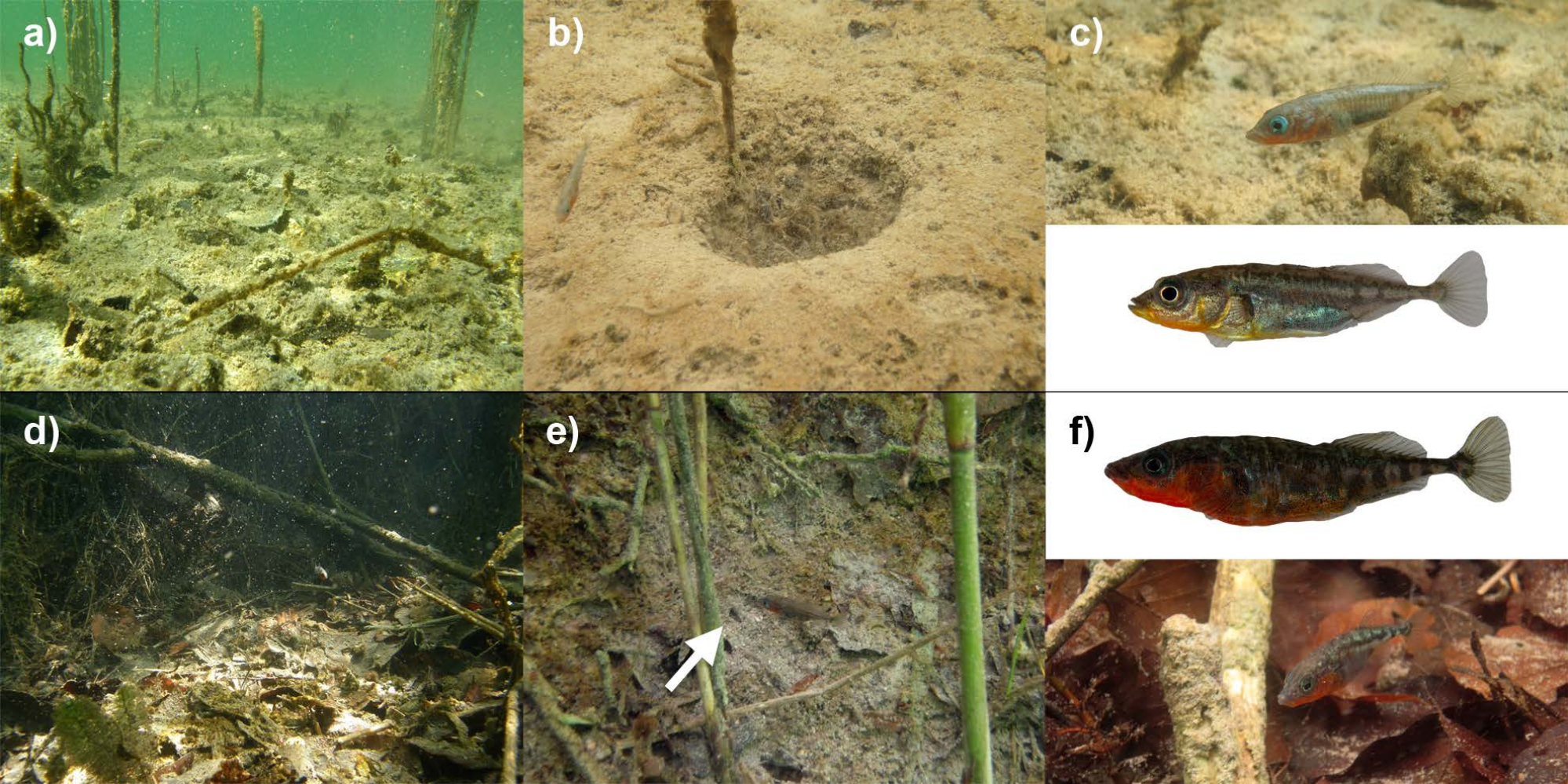
a)
b)
c)
d)
e)
f)

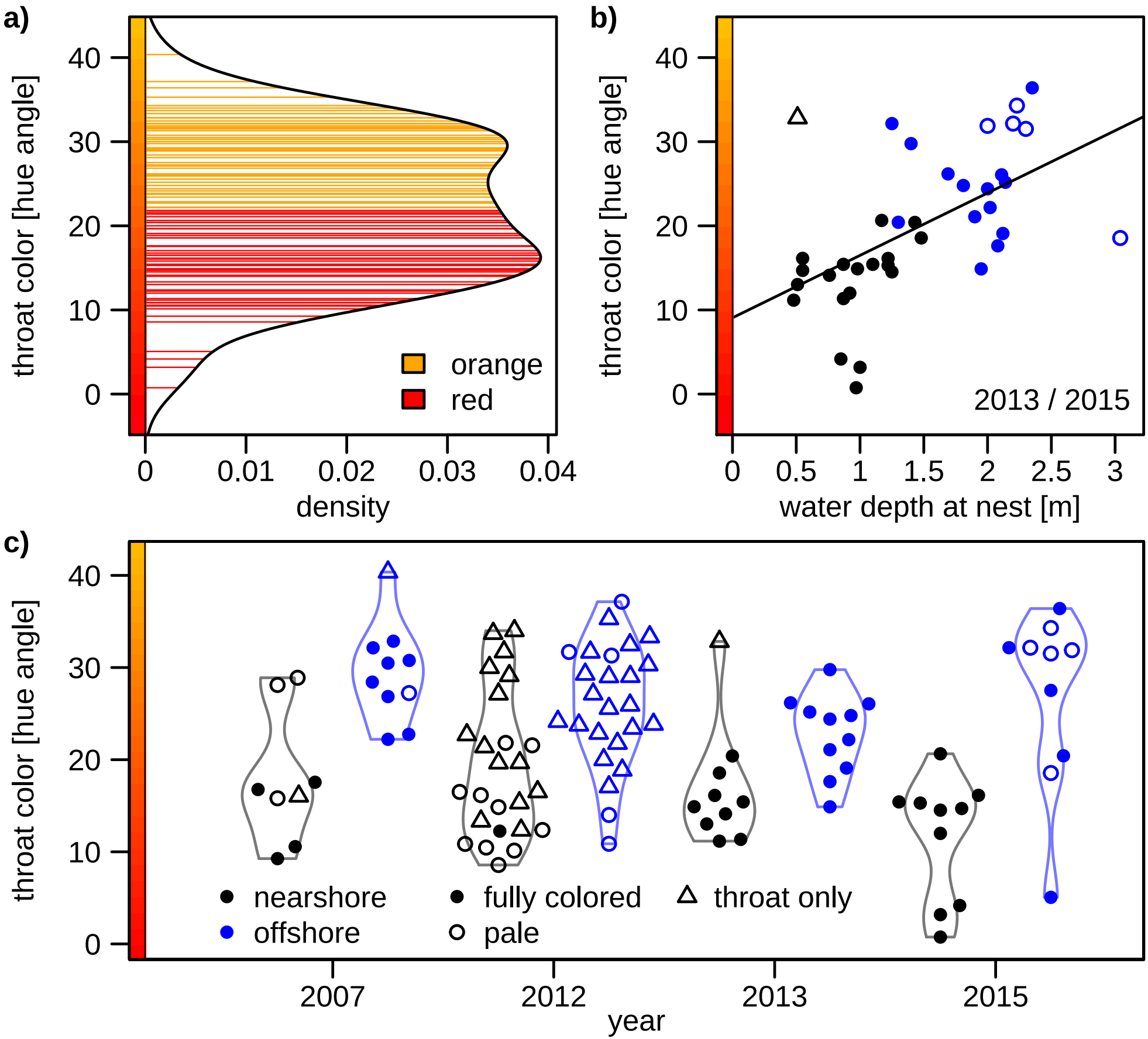
a)
throat color [hue angle]
density
orange
red
b)
throat color [hue angle]
water depth at nest [m]
2013 / 2015
c)
throat color [hue angle]
year
2007
2012
2013
2015
nearshore
offshore
fully colored
pale
throat only

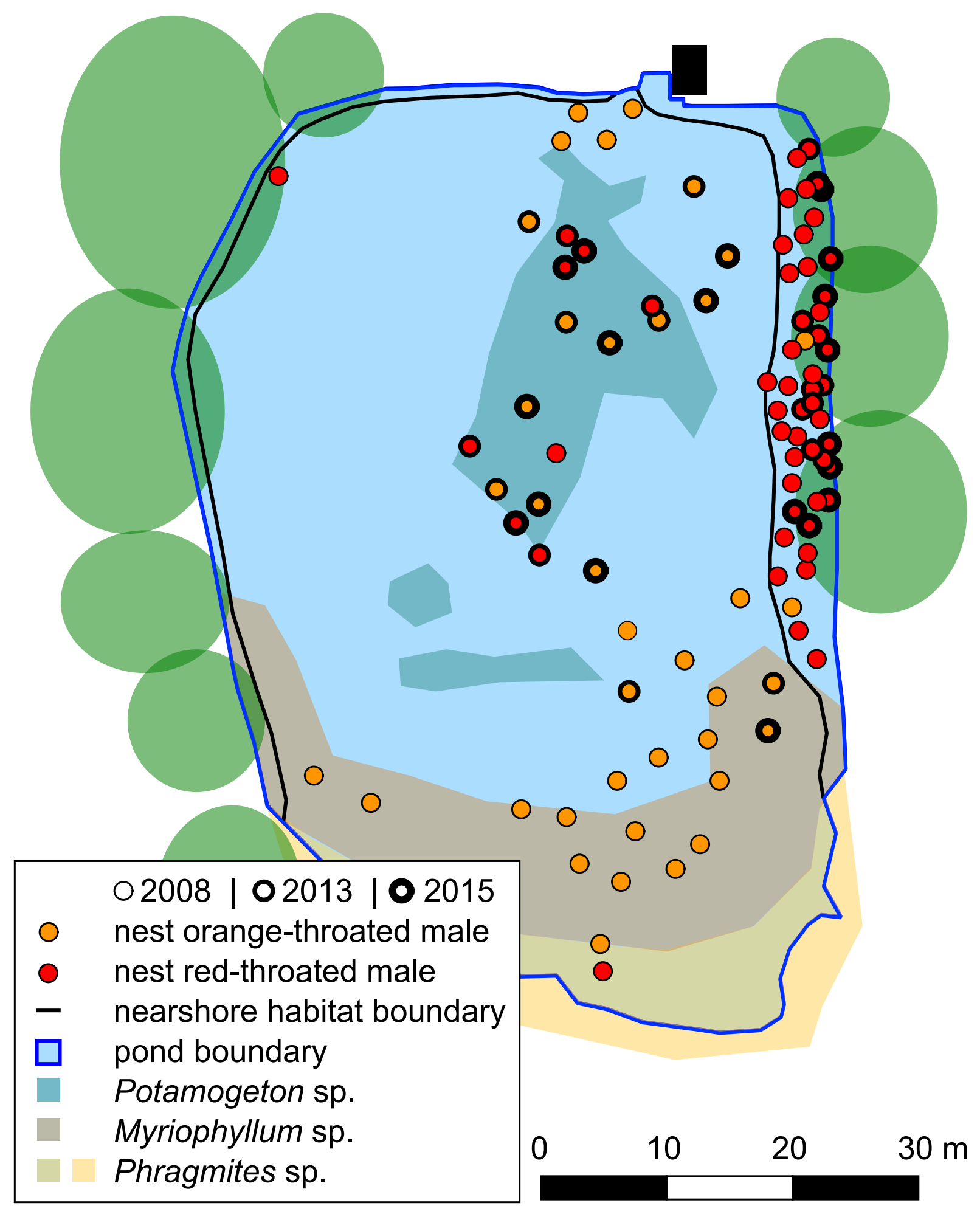
2008 | 2013 | 2015
nest orange-throated male
nest red-throated male
nearshore habitat boundary
pond boundary
Potamogeton sp.
Myriophyllum sp.
Phragmites sp.
0
10
20
30 m

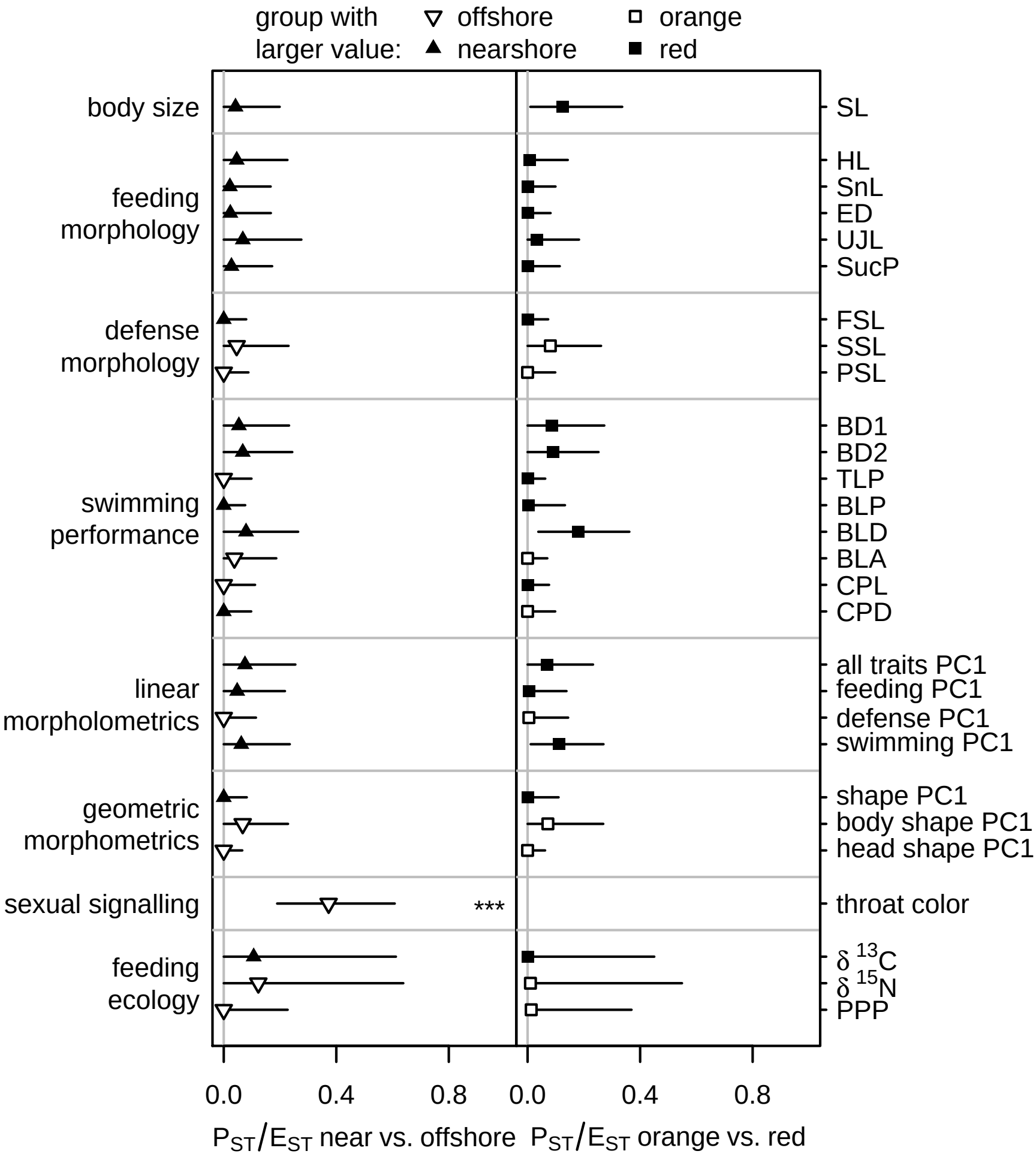
group with larger value:
offshore
nearshore
orange
red
body size
feeding morphology
defense morphology
swimming performance
linear morpholometrics
geometric morphometrics
sexual signalling
feeding ecology
SL
HL
SnL
ED
UJL
SucP
FSL
SSL
PSL
BD1
BD2
TLP
BLP
BLD
BLA
CPL
CPD
all traits PC1
feeding PC1
defense PC1
swimming PC1
shape PC1
body shape PC1
head shape PC1
throat color
δ 13C
δ 15N
PPP
***
0.0
0.4
0.8
0.0
0.4
0.8
PST/EST near vs. offshore
PST/EST orange vs. red

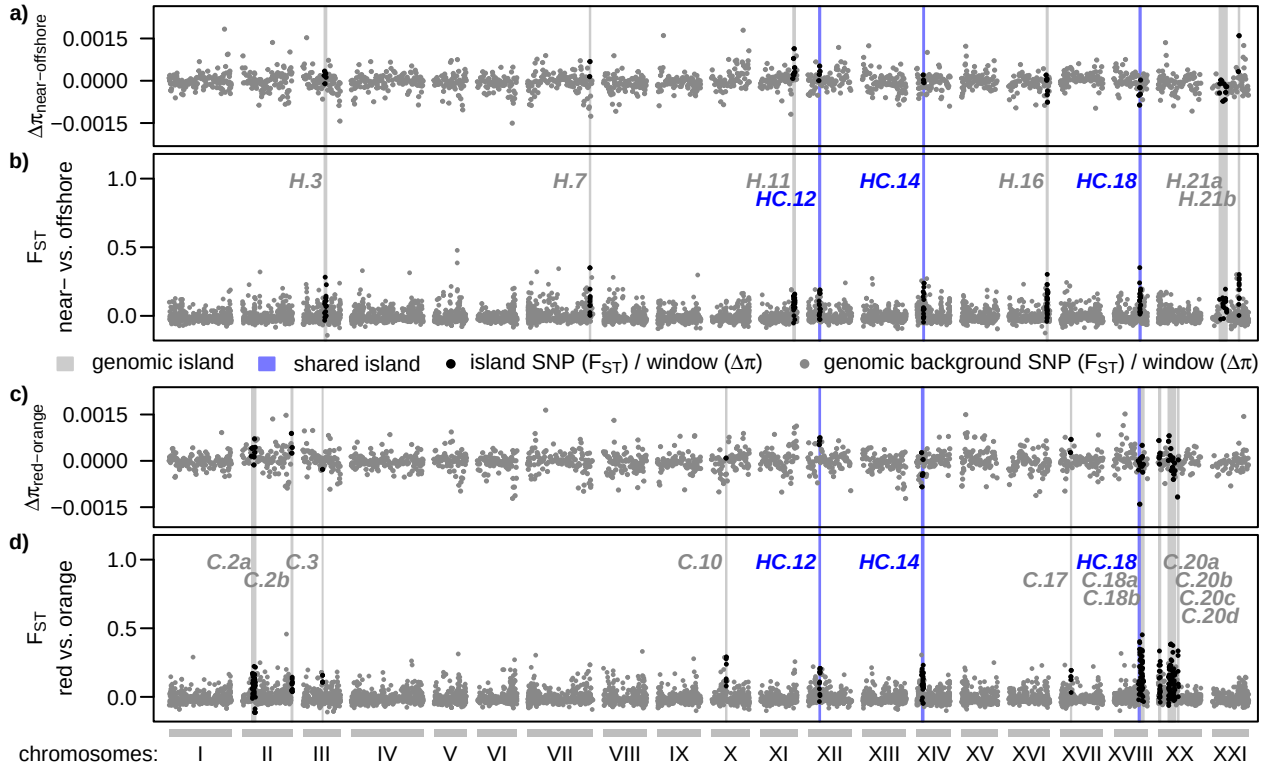
a)
Δπnear−offshore
0.0015
0.0000
−0.0015
b)
FST
near− vs. offshore
1.0
0.5
0.0
H.3
H.7
H.11
HC.12
HC.14
H.16
HC.18
H.21a
H.21b
genomic island
shared island
island SNP (FST) / window (Δπ)
genomic background SNP (FST) / window (Δπ)
c)
Δπred−orange
0.0015
0.0000
−0.0015
d)
FST
red vs. orange
1.0
0.5
0.0
C.2a
C.2b
C.3
C.10
HC.12
HC.14
C.17
HC.18
C.18a
C.18b
C.20a
C.20b
C.20c
C.20d
chromosomes:
I
II
III
IV
V
VI
VII
VIII
IX
X
XI
XII
XIII
XIV
XV
XVI
XVII
XVIII
XX
XXI

Supporting Information

Supplementary Figures

Fig. S1. Linear and geometric morphometric traits measured in this study. We set 19 landmarks (red circles) and measured 17 linear traits (blue bars) as well as throat color (blue circle). See Tab. 1 for trait abbreviations. Suction proxy (SucP) is the distance along the body axes from the anterior-most point of the premaxillary bone to the junction of dorsal and head scales.

Fig. S2. Variation in linear morphometric traits among males grouped by habitat and throat color. a) Residuals of 16 size-corrected linear traits, see Tab. 1 for abbreviations. Nearshore / red-throated males tend to be on average larger-headed and deeper-bodied and show a larger dorsal fin (Tab. 1). b) PCA for the 16 size-corrected linear traits with individuals grouped by throat color and nest habitat. c) Body size distribution of males sampled in 2007, 2013 and 2015. Nearshore / red-throated males tend to be on average larger than offshore / orange males (Tab. 1). Differences in body size between years are likely due to variation in sampling dates and growth rates depending on different winter conditions in these years.

Fig. S3. Variation in body shape among males grouped by habitat and throat color, showing a trend for shorter heads and more slender bodies in offshore / orange males. Grey outlines show body shape at PC/CV=0 and black outlines the respective values indicated by the axis label. a) & b) Principal component analysis results of male overall shape variation. PC axes 2 and 3 are shown, as the first PC axes reflects bending. c) & d) Canonical variance analysis results of male overall shape variation for males grouped into nearshore vs. offshore (c) and red vs. orange (d) males.

Fig. S4. Stomach content and stable isotope data for males from 2007. a) Stomach contents: Offshore / orange males tended to have more copepods and cladocerans, as well as more stickleback eggs in their stomachs, while nearshore / red stickleback had more chironomids and isopods, in line with their proximity to terrestrial habitats. b) & c) Carbon depletion (b) tends to be stronger in nearshore / red stickleback and they tend to occupy an on average higher trophic position (c) than offshore / orange males, however these differences are not significant (Tab. 1).

Supplementary Tables

Table S1. Candidate genes in genomic islands with functions relevant to phenotypic differentiation among Jordeweiher stickleback males.

Island	Gene name	Gene	Ensembl*	Relevant GO terms / GO super-terms
C.2a	insulin-like growth factor 1b receptor	igf1rb	14729	camera-type eye-development, photoreceptor cell maintenance
C.2a	LEO1 homolog, Paf1/RNA polymerase II complex component	leo1	14999	melanocyte differentiation
C.2b	cyclic nucleotide gated channel beta 1a	cngb1a	17581	visual perception
C.2b	forkhead box B1a	foxb1a	17597	visual learning
C.3	RAB18B, member RAS oncogene family	rab18b	16395	eye development
C.3	forkhead box C1a	foxc1a	16468	camera-type eye-development
H.11	recoverin a	rcvrna	14486	cone photoresponse recovery
H.11	granulin a	grna	14616	neural retina development
H.11	ribosomal protein L27	rpl27	14635	erythrocyte differentiation
HC.12	ATPase, H+ transporting, lysosomal accessory protein 1b	atp6ap1b	11378	eye pigment granule organization, melanosome organization, retina development in camera-type eye, retinal pigment epithelium development
HC.12	premelanosome protein b	pmelb	11605	developmental pigmentation, melanosome organization
HC.14	ribosomal protein L7a	rpl7a	15957	embryonic eye morphogenesis
H.16	gap junction protein, alpha 3	gja3	1367	post-embryonic eye morphogenesis
H.16	intraflagellar transport 88 homolog	ift88	1380	eye photoreceptor cell development, photoreceptor cell maintenance
HC.18	RAB32a, member RAS oncogene family	rab32a	11637	melanosome organization
HC.18	ribosomal protein S7	rps7	11913	nucleate erythrocyte
C.18b	opsin 8, group member b	opn8b	12337	G-protein coupled photoreceptor activity, phototransduction
C.20c	glyceraldehyde-3-phosphate dehydrogenase	gapdh	10219	nucleate erythrocyte
C.20c	Ras interacting protein 1	rasip1	10504	nucleate erythrocyte
C.20c	interleukin 11a	il11a	10508	retinal ganglion cell
C.20c	recoverin 2	rcvrn2	10601	cone photoresponse recovery
C.20c	PRP31 pre-mRNA processing factor 31 homolog (yeast)	prpf31	11464	retina development in camera-type eye
C.20c	PRP3 pre-mRNA processing factor 3 homolog (yeast)	prpf3	11792	retina development in camera-type eye
H.21a	RAB18A, member RAS oncogene family	rab18a	1694	eye development
H.21a	Kruppel-like factor 6a	klf6a	1778	erythrocyte maturation

Island	Gene name	Gene	Ensembl*	Relevant GO terms / GO super-terms
H.21a	ATP-binding cassette, sub-family A (ABC1), member 4a	abca4a	2000	visual perception
H.21a	cyclic nucleotide gated channel beta 3	cngb3	2128	visual perception
H.21b	nephronophthisis 3	nphp3	3823	visual perception

*Ensembl-Gene ID, e.g. ENSGACG00000001778 shown as 1778.

Table S2. Table of QTLs and outlier regions identified in previous studies overlapping with genomic islands from this study. PVE: percentage of variance explained, OutR: outlier region.

Type	Chrom.	Start	End	Confidence interval	Trait category	Trait	PVE	Overlapping island	Reference
QTL	chrII	1,554,409	5,248,887	associated marker ± 1 Mb	body shape	landmark x23	9.5	C.2a	Rogers *et al.* 2012
QTL	chrII	2,554,409	13,504,821	1.5-LOD region as reported	feeding	row 2 joint raker number	5.3	C.2a	Miller *et al.* 2014
QTL	chrII	2,554,409	13,504,821	1.5-LOD region as reported	feeding	row 3 epi raker number	6.4	C.2a	Miller *et al.* 2014
QTL	chrII	2,554,409	21,574,761	1.5-LOD region as reported	feeding	joint raker number	4.7	C.2a	Miller *et al.* 2014
QTL	chrII	2,554,409	21,574,761	1.5-LOD region as reported	body shape	non-ray-bearing postanal pterygiophore number	5.5	C.2a	Miller *et al.* 2014
QTL	chrII	4,086,475	7,655,992	1.5-LOD region as reported	feeding	epibranchial 1 length	6.7	C.2a	Miller *et al.* 2014
QTL	chrII	4,248,797	21,574,761	1.5-LOD region as reported	feeding	opercle width	7.5	C.2a	Miller *et al.* 2014
QTL	chrII	4,786,748	21,574,761	1.5-LOD region as reported	defence	dorsal spine 2 length	3.9	C.2a	Miller *et al.* 2014
QTL	chrIII	4,622,006	16,690,554	1.5-LOD region as reported	feeding	premaxilla length	3.7	C.3, H.3	Miller *et al.* 2014
QTL	chrVII	26,760,481	30,314,299	associated marker ± 1 Mb	body shape	landmark x25	12.8	H.7	Rogers *et al.* 2012
QTL	chrVII	26,760,481	30,314,299	associated marker ± 1 Mb	body shape	landmark x24	13.3	H.7	Rogers *et al.* 2012
QTL	chrVII	26,882,412	30,850,397	1.5-LOD region as reported	feeding	premaxilla length	3.9	H.7	Miller *et al.* 2014
QTL	chrVII	27,760,481	30,850,397	1.5-LOD region as reported	feeding	opercle width	5.4	H.7	Miller *et al.* 2014
QTL	chrVII	27,760,481	30,850,397	1.5-LOD region as reported	feeding	dentary height	5.7	H.7	Miller *et al.* 2014
QTL	chrVII	28,313,620	30,314,299	associated marker ± 1 Mb	defence	complete vs. reduced pelvis		H.7	Shapiro *et al.* 2004
QTL	chrVII	28,313,620	30,314,299	associated marker ± 1 Mb	defence	pelvis asymmetry	13.5	H.7	Shapiro *et al.* 2004
QTL	chrVII	28,313,620	30,314,299	associated marker ± 1 Mb	defence	ascending branch height	22.2	H.7	Shapiro *et al.* 2004
QTL	chrVII	28,313,620	30,314,299	associated marker ± 1 Mb	defence	pelvic girdle length	27.8	H.7	Shapiro *et al.* 2004
QTL	chrVII	28,313,620	30,314,299	associated marker ± 1 Mb	defence	pelvic spine length	43.7	H.7	Shapiro *et al.* 2004
QTL	chrVII	28,313,620	30,314,299	associated marker ± 1 Mb	defence	mendelian pelvic locus		H.7	Cresko *et al.* 2004
QTL	chrX	3,320,834	8,666,776	1.5-LOD region as reported	feeding	dorsal toothplate 1 tooth number	4.2	C.10	Miller *et al.* 2014
QTL	chrX	3,320,834	8,666,776	1.5-LOD region as reported	feeding	dorsal toothplate 2 tooth number	7.6	C.10	Miller *et al.* 2014
QTL	chrX	3,320,834	12,662,644	1.5-LOD region as reported	feeding	ventral toothplate tooth number	3.6	C.10	Miller *et al.* 2014
QTL	chrX	3,320,834	12,662,644	1.5-LOD region as reported	body shape	last postanal pterygiophore position	4.4	C.10	Miller *et al.* 2014
QTL	chrX	3,320,834	12,662,644	1.5-LOD region as reported	defence	serration number on dorsal spine 2	6.1	C.10	Miller *et al.* 2014
QTL	chrX	3,320,834	12,662,644	1.5-LOD region as reported	defence	serration area on dorsal spine 2	6.7	C.10	Miller *et al.* 2014
QTL	chrX	3,320,834	16,084,203	1.5-LOD region as reported	feeding	all raker number	3.0	C.10	Miller *et al.* 2014
QTL	chrX	3,962,473	16,084,203	1.5-LOD region as reported	feeding	joint raker number	4.4	C.10	Miller *et al.* 2014
QTL	chrX	5,838,691	7,839,293	associated marker ± 1 Mb	feeding	tooth number	3.3	C.10	Cleves *et al.* 2014
QTL	chrX	6,287,740	16,084,203	1.5-LOD region as reported	feeding	row 6 joint raker number	6.4	C.10	Miller *et al.* 2014
QTL	chrX	6,838,691	16,084,203	1.5-LOD region as reported	feeding	row 7 hypo raker number	5.5	C.10	Miller *et al.* 2014

Type	Chrom.	Start	End	Confidence interval	Trait category	Trait	PVE	Overlapping island	Reference
QTL	chrXII	498,629	9,007,257	associated marker ± 1 Mb	body shape	landmark y12	9.0	HC.12	Rogers *et al.* 2012
QTL	chrXII	498,629	9,007,257	associated marker ± 1 Mb	body shape	body depth	9.0	HC.12	Rogers *et al.* 2012
QTL	chrXII	498,629	9,007,257	associated marker ± 1 Mb	body shape	landmark y6	11.0	HC.12	Rogers *et al.* 2012
QTL	chrXII	3,528,005	15,130,396	1.5-LOD region as reported	feeding	opercle neck width	8.4	HC.12	Miller *et al.* 2014
QTL	chrXII	3,528,005	19,667,912	1.5-LOD region as reported	feeding	dorsal toothplate 1 width	5.2	HC.12	Miller *et al.* 2014
QTL	chrXII	3,830,036	11,751,243	1.5-LOD region as reported	feeding	ceratobranchial 4 length	3.5	HC.12	Miller *et al.* 2014
QTL	chrXII	3,830,036	19,667,912	1.5-LOD region as reported	feeding	dentary height	6.9	HC.12	Miller *et al.* 2014
QTL	chrXII	3,830,195	5,551,755	1.5-LOD region as reported	feeding	dorsal toothplate 2 width	4.4	HC.12	Miller *et al.* 2014
QTL	chrXII	4,551,614	6,551,755	associated marker ± 1 Mb	body shape	landmark x25	11.1	HC.12	Rogers *et al.* 2012
QTL	chrXII	5,551,749	15,130,396	1.5-LOD region as reported	feeding	premaxilla length	3.7	HC.12	Miller *et al.* 2014
QTL	chrXIV	1	12,440,728	1.5-LOD region as reported	feeding	in-lever 1 of articular length	5.3	HC.14	Miller *et al.* 2014
QTL	chrXIV	2,698,856	9,939,598	1.5-LOD region as reported	feeding	epibranchial 1 length	4.0	HC.14	Miller *et al.* 2014
QTL	chrXIV	2,698,856	15,188,529	1.5-LOD region as reported	feeding	ceratobranchial 1 length	3.5	HC.14	Miller *et al.* 2014
QTL	chrXIV	2,698,856	15,188,529	1.5-LOD region as reported	feeding	ceratobranchial 4 length	3.6	HC.14	Miller *et al.* 2014
QTL	chrXIV	2,698,856	15,188,529	1.5-LOD region as reported	feeding	ceratobranchial 5 length	3.7	HC.14	Miller *et al.* 2014
QTL	chrXIV	2,698,856	15,188,529	1.5-LOD region as reported	feeding	premaxilla length	3.8	HC.14	Miller *et al.* 2014
QTL	chrXIV	2,698,856	15,188,529	1.5-LOD region as reported	feeding	articular length	3.9	HC.14	Miller *et al.* 2014
QTL	chrXIV	2,698,856	15,188,529	1.5-LOD region as reported	feeding	premaxilla height	5.2	HC.14	Miller *et al.* 2014
QTL	chrXVI	16,413,003	18,202,793	1.5-LOD region as reported	feeding	medial gill raker length	6.0	H.16	Glazer *et al.* 2015
QTL	chrXVI	16,413,003	18,202,793	1.5-LOD region as reported	feeding	lateral gill raker length	6.3	H.16	Glazer *et al.* 2015
QTL	chrXVI	16,413,003	18,202,793	1.5-LOD region as reported	feeding	middle gill raker length	9.1	H.16	Glazer *et al.* 2015
QTL	chrXVII	763,556	16,509,762	associated marker ± 1 Mb	body shape	landmark x25	9.5	C.17	Rogers *et al.* 2012
QTL	chrXVII	2,058,474	5,290,116	1.5-LOD region as reported	feeding	ceratobranchial 1 length	3.7	C.17	Miller *et al.* 2014
QTL	chrXVII	2,058,474	5,290,116	1.5-LOD region as reported	feeding	ceratobranchial 3 length	4.1	C.17	Miller *et al.* 2014
QTL	chrXVII	2,058,474	5,290,116	1.5-LOD region as reported	feeding	hypo raker number	5.1	C.17	Miller *et al.* 2014
QTL	chrXVII	2,058,474	15,509,762	1.5-LOD region as reported	feeding	dentary height	4.6	C.17	Miller *et al.* 2014
QTL	chrXVII	2,058,474	15,509,762	1.5-LOD region as reported	feeding	ceratobranchial 2 length	4.9	C.17	Miller *et al.* 2014
QTL	chrXVII	2,058,474	15,509,762	1.5-LOD region as reported	feeding	dentary length	7.5	C.17	Miller *et al.* 2014
QTL	chrXVII	2,058,474	20,254,136	1.5-LOD region as reported	feeding	middle raker spacing	3.3	C.17	Miller *et al.* 2014
QTL	chrXVII	4,466,582	17,136,436	1.5-LOD region as reported	feeding	ventral tooth plate tooth number	7.3	C.17	Ellis *et al.* 2015
QTL	chrXVIII	5,070,409	12,934,334	1.5-LOD region as reported	feeding	ventral tooth plate intertooth spacing	9.9	HC.18	Ellis *et al.* 2015
QTL	chrXVIII	7,613,260	15,688,949	1.5-LOD region as reported	feeding	all raker number	2.8	HC.18, C.18a, C.18b	Miller *et al.* 2014
QTL	chrXVIII	9,393,393	12,520,434	1.5-LOD region as reported	body shape	frontal width	3.8	HC.18	Miller *et al.* 2014

Type	Chrom.	Start	End	Confidence interval	Trait category	Trait	PVE	Overlapping island	Reference
QTL	chrXVIII	9,393,393	14,194,268	1.5-LOD region as reported	feeding	ceratobranchial 1 length	2.9	HC.18, C.18a, C.18b	Miller *et al.* 2014
QTL	chrXVIII	11,520,276	13,520,434	associated marker ± 1 Mb	body shape	body shape:dorsal extent of the ascending branch of the pelvis (x)	4.5	HC.18, C.18a, C.18b	Albert *et al.* 2008
QTL	chrXVIII	11,520,276	13,520,434	associated marker ± 1 Mb	body shape	body shape:dorsal extent of ectocorocoid (x)	5.5	HC.18, C.18a, C.18b	Albert *et al.* 2008
QTL	chrXVIII	11,520,276	13,520,434	associated marker ± 1 Mb	body shape	body shape:posterior extent of ectocorocoid (x)	5.7	HC.18, C.18a, C.18b	Albert *et al.* 2008
QTL	chrXVIII	11,520,276	13,520,434	associated marker ± 1 Mb	body shape	body shape:anterior extent of ectocorocoid (y)	5.7	HC.18, C.18a, C.18b	Albert *et al.* 2008
QTL	chrXVIII	11,520,276	13,520,434	associated marker ± 1 Mb	body shape	body shape:posterior extent of premaxilla (x)	6.3	HC.18, C.18a, C.18b	Albert *et al.* 2008
QTL	chrXX	3,763,571	15,500,733	1.5-LOD region as reported	feeding	lateral gill raker length	6.5	C.20b, C.20c, C.20d	Glazer *et al.* 2015
QTL	chrXX	3,806,402	15,047,247	1.5-LOD region as reported	feeding	gill raker number adult	11.5	C.20b, C.20c, C.20d	Glazer *et al.* 2014
QTL	chrXX	3,806,402	19,341,384	1.5-LOD region as reported	feeding	gill raker number adult	9.7	C.20b, C.20c, C.20d	Glazer *et al.* 2014
QTL	chrXX	3,831,311	16,942,924	associated marker ± 1 Mb	defence	pelvic girdle length	11.7	C.20b, C.20c, C.20d	Rogers *et al.* 2012
QTL	chrXX	4,831,311	7,907,076	1.5-LOD region as reported	feeding	all raker number	18.1	C.20b, C.20c	Miller *et al.* 2014
QTL	chrXX	4,831,311	11,260,235	1.5-LOD region as reported	feeding	row 1 raker number	8.6	C.20b, C.20c, C.20d	Miller *et al.* 2014
QTL	chrXX	4,831,311	11,260,235	1.5-LOD region as reported	feeding	branchial arch 1 raker number	11.0	C.20b, C.20c, C.20d	Miller *et al.* 2014
QTL	chrXX	4,831,311	12,244,188	1.5-LOD region as reported	defence	anal spine length	6.4	C.20b, C.20c, C.20d	Miller *et al.* 2014
QTL	chrXX	4,831,311	12,244,188	1.5-LOD region as reported	feeding	branchial arch 2 raker number	13.6	C.20b, C.20c, C.20d	Miller *et al.* 2014
QTL	chrXX	4,831,311	12,244,188	1.5-LOD region as reported	feeding	odd row raker number	15.5	C.20b, C.20c, C.20d	Miller *et al.* 2014
QTL	chrXX	4,831,311	12,244,188	1.5-LOD region as reported	feeding	cerato raker number	25.3	C.20b, C.20c, C.20d	Miller *et al.* 2014
QTL	chrXX	4,831,311	16,175,213	1.5-LOD region as reported	body shape	frontal width	3.2	C.20b, C.20c, C.20d	Miller *et al.* 2014
QTL	chrXX	4,831,311	16,175,213	1.5-LOD region as reported	defence	dorsal spine 2 area	4.7	C.20b, C.20c, C.20d	Miller *et al.* 2014
QTL	chrXX	4,831,311	16,175,213	1.5-LOD region as reported	feeding	row 2 raker number	7.4	C.20b, C.20c, C.20d	Miller *et al.* 2014
QTL	chrXX	4,831,311	16,175,213	1.5-LOD region as reported	feeding	dorsal toothplate 2 tooth number	7.6	C.20b, C.20c, C.20d	Miller *et al.* 2014
QTL	chrXX	4,831,311	16,175,213	1.5-LOD region as reported	feeding	dorsal toothplate 1 tooth number	8.8	C.20b, C.20c, C.20d	Miller *et al.* 2014
QTL	chrXX	4,831,311	16,175,213	1.5-LOD region as reported	feeding	row 4 raker number	10.2	C.20b, C.20c, C.20d	Miller *et al.* 2014
QTL	chrXX	4,831,311	16,175,213	1.5-LOD region as reported	feeding	row 4 cerato raker number	11.5	C.20b, C.20c, C.20d	Miller *et al.* 2014
QTL	chrXX	4,831,311	16,175,213	1.5-LOD region as reported	feeding	row 5 raker number	11.6	C.20b, C.20c, C.20d	Miller *et al.* 2014
QTL	chrXX	4,831,311	16,175,213	1.5-LOD region as reported	feeding	row 6 cerato raker number	11.7	C.20b, C.20c, C.20d	Miller *et al.* 2014
QTL	chrXX	4,831,311	16,175,213	1.5-LOD region as reported	feeding	row 3 raker number	12.4	C.20b, C.20c, C.20d	Miller *et al.* 2014
QTL	chrXX	4,831,311	16,175,213	1.5-LOD region as reported	feeding	lateral raker spacing	12.5	C.20b, C.20c, C.20d	Miller *et al.* 2014
QTL	chrXX	4,831,311	16,175,213	1.5-LOD region as reported	feeding	row 5 cerato raker number	13.0	C.20b, C.20c, C.20d	Miller *et al.* 2014

Type	Chrom.	Start	End	Confidence interval	Trait category	Trait	PVE	Overlapping island	Reference
QTL	chrXX	4,831,311	16,175,213	1.5-LOD region as reported	feeding	row 9 cerato raker number	13.2	C.20b, C.20c, C.20d	Miller *et al.* 2014
QTL	chrXX	4,831,311	16,175,213	1.5-LOD region as reported	feeding	row 2 cerato raker number	13.4	C.20b, C.20c, C.20d	Miller *et al.* 2014
QTL	chrXX	4,831,311	16,175,213	1.5-LOD region as reported	feeding	row 7 cerato raker number	13.4	C.20b, C.20c, C.20d	Miller *et al.* 2014
QTL	chrXX	4,831,311	16,175,213	1.5-LOD region as reported	feeding	row 6 raker number	13.7	C.20b, C.20c, C.20d	Miller *et al.* 2014
QTL	chrXX	4,831,311	16,175,213	1.5-LOD region as reported	feeding	row 1 cerato raker number	14.3	C.20b, C.20c, C.20d	Miller *et al.* 2014
QTL	chrXX	4,831,311	16,175,213	1.5-LOD region as reported	feeding	middle raker spacing	14.8	C.20b, C.20c, C.20d	Miller *et al.* 2014
QTL	chrXX	4,831,311	16,175,213	1.5-LOD region as reported	feeding	even row raker number	16.4	C.20b, C.20c, C.20d	Miller *et al.* 2014
QTL	chrXX	4,831,311	16,175,213	1.5-LOD region as reported	body shape	supraoccipital crest width	16.6	C.20b, C.20c, C.20d	Miller *et al.* 2014
QTL	chrXX	4,831,311	16,175,213	1.5-LOD region as reported	feeding	row 3 cerato raker number	16.9	C.20b, C.20c, C.20d	Miller *et al.* 2014
QTL	chrXX	4,831,311	16,175,213	1.5-LOD region as reported	feeding	branchial arch 3 raker number	17.5	C.20b, C.20c, C.20d	Miller *et al.* 2014
QTL	chrXX	4,831,311	16,433,340	1.5-LOD region as reported	feeding	row 8 raker number	7.5	C.20b, C.20c, C.20d	Miller *et al.* 2014
QTL	chrXX	4,831,311	18,002,157	1.5-LOD region as reported	defence	dorsal spine 3 length	3.5	C.20b, C.20c, C.20d	Miller *et al.* 2014
QTL	chrXX	4,831,311	18,002,157	1.5-LOD region as reported	feeding	premaxilla height	4.5	C.20b, C.20c, C.20d	Miller *et al.* 2014
QTL	chrXX	4,831,311	18,002,157	1.5-LOD region as reported	feeding	ventral toothplate width	5.0	C.20b, C.20c, C.20d	Miller *et al.* 2014
QTL	chrXX	4,831,311	18,002,157	1.5-LOD region as reported	body shape	vertebrae number	5.2	C.20b, C.20c, C.20d	Miller *et al.* 2014
QTL	chrXX	4,831,311	18,002,157	1.5-LOD region as reported	defence	serration number on dorsal spine 2	8.0	C.20b, C.20c, C.20d	Miller *et al.* 2014
QTL	chrXX	4,831,311	18,002,157	1.5-LOD region as reported	feeding	branchial arch 4 raker number	8.1	C.20b, C.20c, C.20d	Miller *et al.* 2014
QTL	chrXX	4,831,311	18,002,157	1.5-LOD region as reported	defence	serration area on dorsal spine 2	9.0	C.20b, C.20c, C.20d	Miller *et al.* 2014
QTL	chrXX	6,027,562	15,047,247	1.5-LOD region as reported	feeding	gill raker number adult	22.4	C.20b, C.20c, C.20d	Glazer *et al.* 2014
QTL	chrXX	6,907,076	8,907,472	associated marker ± 1 Mb	body shape	landmark y27	9.3	C.20c	Rogers *et al.* 2012
QTL	chrXX	8,194,876	18,002,157	1.5-LOD region as reported	feeding	ventral toothplate tooth number	5.4	C.20d	Miller *et al.* 2014
QTL	chrXXI	1,811,555	3,811,729	associated marker ± 1 Mb	body shape	landmark y26	10.0	H.21a	Rogers *et al.* 2012
QTL	chrXXI	1,811,555	3,811,729	associated marker ± 1 Mb	body shape	landmark y25	10.6	H.21a	Rogers *et al.* 2012
QTL	chrXXI	1,811,555	3,811,729	associated marker ± 1 Mb	defence	plate number in aa f2s	23.2	H.21a	Colosimo *et al.* 2004
QTL	chrXXI	2,811,555	9,041,896	1.5-LOD region as reported	body shape	third predorsal pterygiophore position	5.4	H.21a	Miller *et al.* 2014
QTL	chrXXI	2,811,555	13,187,908	1.5-LOD region as reported	defence	dorsal spine 2 length	3.0	H.21a, H.21b	Miller *et al.* 2014
QTL	chrXXI	2,811,555	13,187,908	1.5-LOD region as reported	feeding	ceratobranchial 1 length	3.0	H.21a, H.21b	Miller *et al.* 2014
QTL	chrXXI	2,811,555	13,187,908	1.5-LOD region as reported	feeding	hypo raker number	4.2	H.21a, H.21b	Miller *et al.* 2014
QTL	chrXXI	2,811,555	13,187,908	1.5-LOD region as reported	feeding	ceratobranchial 3 length	4.3	H.21a, H.21b	Miller *et al.* 2014
QTL	chrXXI	2,811,555	13,187,908	1.5-LOD region as reported	body shape	frontal width	4.9	H.21a, H.21b	Miller *et al.* 2014
QTL	chrXXI	2,811,555	13,187,908	1.5-LOD region as reported	defence	dorsal spine 1 length	5.0	H.21a, H.21b	Miller *et al.* 2014
QTL	chrXXI	2,811,555	13,187,908	1.5-LOD region as reported	feeding	in-lever 2 of articular length	5.3	H.21a, H.21b	Miller *et al.* 2014
QTL	chrXXI	2,811,555	13,187,908	1.5-LOD region as reported	feeding	articular length	5.8	H.21a, H.21b	Miller *et al.* 2014
QTL	chrXXI	2,811,555	13,187,908	1.5-LOD region as reported	feeding	ceratobranchial 4 length	5.9	H.21a, H.21b	Miller *et al.* 2014

Type	Chrom.	Start	End	Confidence interval	Trait category	Trait	PVE	Overlapping island	Reference
QTL	chrXXI	2,811,555	13,187,908	1.5-LOD region as reported	body shape	total postanal pterygiophore number	5.9	H.21a, H.21b	Miller *et al.* 2014
QTL	chrXXI	2,811,555	13,187,908	1.5-LOD region as reported	body shape	last postdorsal pterygiophore position	6.3	H.21a, H.21b	Miller *et al.* 2014
QTL	chrXXI	2,811,555	13,187,908	1.5-LOD region as reported	feeding	dorsal toothplate 1 width	6.5	H.21a, H.21b	Miller *et al.* 2014
QTL	chrXXI	2,811,555	13,187,908	1.5-LOD region as reported	feeding	ceratobranchial 5 length	6.5	H.21a, H.21b	Miller *et al.* 2014
QTL	chrXXI	2,811,555	13,187,908	1.5-LOD region as reported	defence	dorsal spine 3 length	6.7	H.21a, H.21b	Miller *et al.* 2014
QTL	chrXXI	2,811,555	13,187,908	1.5-LOD region as reported	feeding	premaxilla length	7.2	H.21a, H.21b	Miller *et al.* 2014
QTL	chrXXI	2,811,555	13,187,908	1.5-LOD region as reported	feeding	dentary length	7.2	H.21a, H.21b	Miller *et al.* 2014
QTL	chrXXI	2,811,555	13,187,908	1.5-LOD region as reported	feeding	ventral toothplate length	10.7	H.21a, H.21b	Miller *et al.* 2014
QTL	chrXXI	2,811,555	13,187,908	1.5-LOD region as reported	feeding	premaxilla height	12.3	H.21a, H.21b	Miller *et al.* 2014
QTL	chrXXI	2,811,555	13,187,908	1.5-LOD region as reported	feeding	epibranchial 1 length	15.5	H.21a, H.21b	Miller *et al.* 2014
QTL	chrXXI	2,969,125	4,969,333	associated marker ± 1 Mb	defence	lateral plate number	10.0	H.21a	Peichel *et al.* 2001
QTL	chrXXI	2,969,333	9,021,249	associated marker ± 1 Mb	defence	lateral plate-b qtl		H.21a	Cresko *et al.* 2004
QTL	chrXXI	3,930,309	5,930,456	associated marker ± 1 Mb	feeding	tooth plate area	14.7	H.21a	Cleves *et al.* 2014
QTL	chrXXI	4,642,714	14,055,502	1.5-LOD region as reported	feeding	epibranchial 1 length	6.7	H.21a, H.21b	Erickson *et al.* 2014
QTL	chrXXI	4,930,309	13,187,908	1.5-LOD region as reported	feeding	dorsal toothplate 1 tooth number	7.3	H.21a, H.21b	Miller *et al.* 2014
QTL	chrXXI	4,939,045	6,939,294	associated marker ± 1 Mb	feeding	tooth spacing	7.3	H.21a	Cleves *et al.* 2014
QTL	chrXXI	5,777,108	13,187,908	1.5-LOD region as reported	feeding	epibranchial 1 length	9.3	H.21a, H.21b	Erickson *et al.* 2014
QTL	chrXXI	5,939,045	13,187,908	1.5-LOD region as reported	body shape	last postanal pterygiophore position	12.3	H.21a, H.21b	Miller *et al.* 2014
QTL	chrXXI	5,939,045	13,187,908	1.5-LOD region as reported	feeding	dorsal toothplate 2 width	15.4	H.21a, H.21b	Miller *et al.* 2014
QTL	chrXXI	5,939,045	13,187,908	1.5-LOD region as reported	feeding	ventral toothplate tooth number	26.2	H.21a, H.21b	Miller *et al.* 2014
QTL	chrXXI	6,709,145	9,264,690	95% confidence interval as reported	feeding	tooth number	31.5	H.21a	Cleves *et al.* 2014
QTL	chrXXI	7,914,244	13,187,908	1.5-LOD region as reported	feeding	ventral toothplate width	23.6	H.21b	Miller *et al.* 2014
QTL	chrXXI	8,072,478	12,912,828	1.5-LOD region as reported	feeding	ventral tooth plate tooth number	13.5	H.21b	Ellis *et al.* 2015
QTL	chrXXI	9,041,658	13,187,908	1.5-LOD region as reported	feeding	dorsal toothplate 2 tooth number	7.8	H.21b	Miller *et al.* 2014
OutR	chrII	4,879,721	4,895,041	exact region as reported				C.2a	Feulner *et al.* 2015
OutR	chrII	4,968,220	4,994,219	exact region as reported				C.2a	Feulner *et al.* 2015
OutR	chrII	5,130,902	5,156,901	exact region as reported				C.2a	Feulner *et al.* 2015
OutR	chrII	22,113,185	23,708,229	outlier microsat ± 1 Mb				C.2b	Mäkinen *et al.* 2008
OutR	chrII	23,642,336	23,672,335	exact region as reported				C.2b	Feulner *et al.* 2015
OutR	chrIII	7,925,000	9,936,000	outlier microsat ± 1 Mb				C.3	DeFaveri *et al.* 2011
OutR	chrIII	10,209,638	10,288,125	exact region as reported				H.3	Feulner *et al.* 2015
OutR	chrIII	10,256,795	10,270,838	exact region as reported				H.3	Feulner *et al.* 2015
OutR	chrIII	10,260,001	10,270,000	exact region as reported				H.3	Feulner *et al.* 2015

Type	Chrom.	Start	End	Confidence interval	Trait category	Trait	PVE	Overlapping island	Reference
OutR	chrIII	10,298,113	10,326,112	exact region as reported				H.3	Feulner *et al.* 2015
OutR	chrIII	10,423,312	10,498,345	exact region as reported				H.3	Feulner *et al.* 2015
OutR	chrIII	10,600,650	10,625,505	exact region as reported				H.3	Feulner *et al.* 2015
OutR	chrIII	10,626,713	10,750,873	exact region as reported				H.3	Feulner *et al.* 2015
OutR	chrIII	10,805,589	10,830,135	exact region as reported				H.3	Feulner *et al.* 2015
OutR	chrIII	10,849,624	10,934,254	exact region as reported				H.3	Feulner *et al.* 2015
OutR	chrVII	28,101,770	30,101,909	outlier microsat ± 1 Mb				H.7	Mäkinen *et al.* 2008
OutR	chrVII	29,357,287	30,850,397	outlier microsat ± 1 Mb				H.7	Mäkinen *et al.* 2008
OutR	chrXI	14,309,864	16,310,001	outlier microsat ± 1 Mb				H.11	DeFaveri *et al.* 2011
OutR	chrXI	16,359,445	17,646,579	outlier microsat ± 1 Mb				H.11	Kaeuffer *et al.* 2011
OutR	chrXII	4,329,168	18,644,933	exact region as reported				HC.12	Feulner *et al.* 2015
OutR	chrXII	5,330,664	5,365,913	exact region as reported				HC.12	Feulner *et al.* 2015
OutR	chrXII	5,756,782	5,777,305	exact region as reported				HC.12	Marques *et al.* 2016
OutR	chrXVII	4,945,848	4,971,907	exact region as reported				C.17	Feulner *et al.* 2015
OutR	chrXVIII	334,676	15,953,870	exact region as reported				HC.18, C.18a, C.18b	Feulner *et al.* 2015
OutR	chrXX	1	1,570,921	outlier microsat ± 1 Mb				C.20a	DeFaveri *et al.* 2011
OutR	chrXX	618,036	639,311	exact region as reported				C.20a	Jones *et al.* 2012
OutR	chrXX	654,064	660,088	exact region as reported				C.20a	Jones *et al.* 2012
OutR	chrXX	669,147	672,859	exact region as reported				C.20a	Jones *et al.* 2012
OutR	chrXX	674,015	686,169	exact region as reported				C.20a	Jones *et al.* 2012
OutR	chrXX	1,569,221	18,771,174	exact region as reported				C.20b, C.20c, C.20d	Feulner *et al.* 2015
OutR	chrXX	3,830,764	12,260,847	outlier microsat ± 1 Mb		species diagnostic marker		C.20b, C.20c, C.20d	Malek *et al.* 2012
OutR	chrXX	5,229,935	5,265,934	exact region as reported				C.20b	Feulner *et al.* 2015
OutR	chrXX	5,534,011	5,536,418	exact region as reported				C.20b	Jones *et al.* 2012
OutR	chrXX	5,537,509	5,539,221	exact region as reported				C.20b	Jones *et al.* 2012
OutR	chrXX	5,738,160	5,776,342	exact region as reported				C.20b	Feulner *et al.* 2015
OutR	chrXX	5,880,398	5,885,735	exact region as reported				C.20b	Jones *et al.* 2012
OutR	chrXX	6,030,687	6,034,687	exact region as reported				C.20b	Jones *et al.* 2012
OutR	chrXX	6,082,919	6,233,437	exact region as reported				C.20b	Feulner *et al.* 2015
OutR	chrXX	6,929,309	6,940,558	exact region as reported				C.20c	Feulner *et al.* 2015
OutR	chrXX	6,980,238	7,007,237	exact region as reported				C.20c	Feulner *et al.* 2015
OutR	chrXX	6,987,798	7,014,797	exact region as reported				C.20c	Feulner *et al.* 2015
OutR	chrXX	6,993,687	7,003,686	exact region as reported				C.20c	Feulner *et al.* 2015
OutR	chrXX	7,029,059	7,075,058	exact region as reported				C.20c	Feulner *et al.* 2015

Type	Chrom.	Start	End	Confidence interval	Trait category	Trait	PVE	Overlapping island	Reference
OutR	chrXX	7,338,374	7,360,411	exact region as reported				C.20c	Feulner *et al.* 2015
OutR	chrXX	7,357,075	7,420,074	exact region as reported				C.20c	Feulner *et al.* 2015
OutR	chrXX	7,691,924	7,794,108	exact region as reported				C.20c	Feulner *et al.* 2015
OutR	chrXX	7,754,461	7,817,481	exact region as reported				C.20c	Feulner *et al.* 2015
OutR	chrXX	7,886,470	7,921,469	exact region as reported				C.20c	Feulner *et al.* 2015
OutR	chrXX	7,899,308	7,905,715	exact region as reported				C.20c	Jones *et al.* 2012
OutR	chrXX	7,924,665	7,937,687	exact region as reported				C.20c	Jones *et al.* 2012
OutR	chrXX	7,939,687	7,942,187	exact region as reported				C.20c	Jones *et al.* 2012
OutR	chrXX	7,955,271	8,000,270	exact region as reported				C.20c	Feulner *et al.* 2015
OutR	chrXX	8,003,537	10,004,159	outlier microsat ± 1 Mb				C.20c, C.20d	Mäkinen *et al.* 2008
OutR	chrXXI	4,900,560	4,918,709	exact region as reported				H.21a	Jones *et al.* 2012
OutR	chrXXI	4,920,167	4,928,691	exact region as reported				H.21a	Jones *et al.* 2012
OutR	chrXXI	5,361,805	5,378,230	exact region as reported				H.21a	Feulner *et al.* 2015
OutR	chrXXI	5,573,572	5,684,081	exact region as reported				H.21a	Feulner *et al.* 2015
OutR	chrXXI	5,655,189	5,676,188	exact region as reported				H.21a	Feulner *et al.* 2015
OutR	chrXXI	5,664,149	5,674,148	exact region as reported				H.21a	Feulner *et al.* 2015
OutR	chrXXI	5,768,854	5,951,853	exact region as reported				H.21a	Feulner *et al.* 2015
OutR	chrXXI	6,100,266	6,276,857	exact region as reported				H.21a	Feulner *et al.* 2015
OutR	chrXXI	6,868,953	6,951,952	exact region as reported				H.21a	Feulner *et al.* 2015

Note that the genomic coordinates are based on the re-assembly reference genome (Glazer et al. 2015).

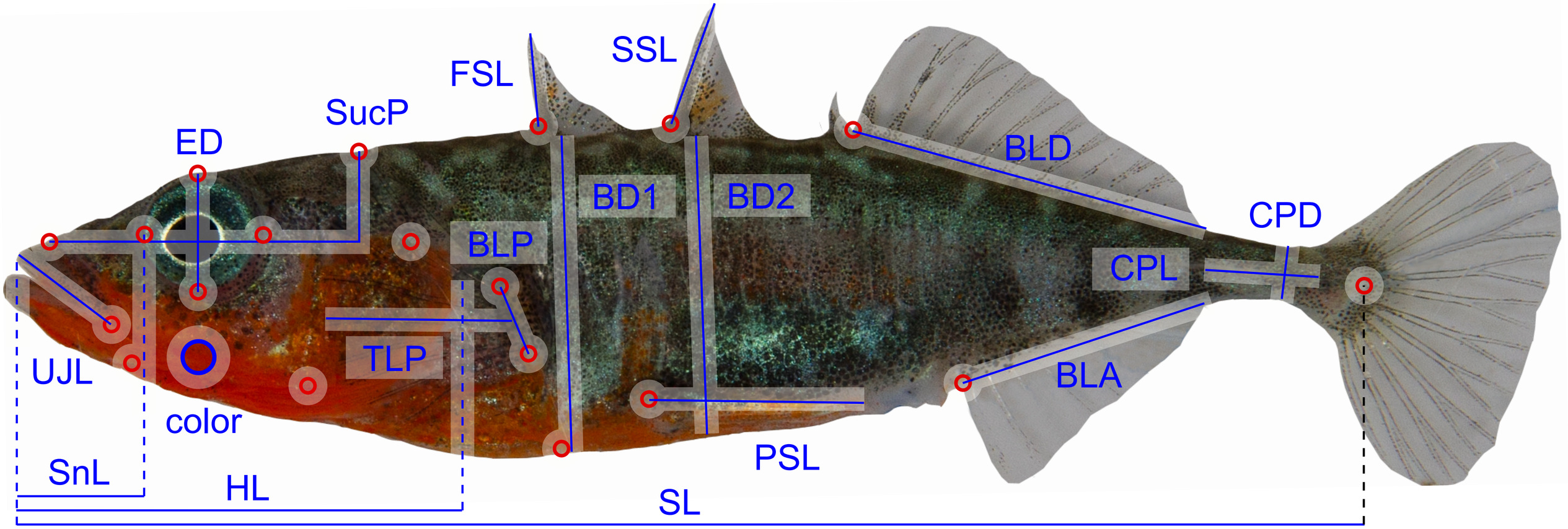
FSL
SSL
SucP
ED
BLD
BD1
BD2
CPD
BLP
CPL
TLP
UJL
BLA
color
PSL
SnL
HL
SL

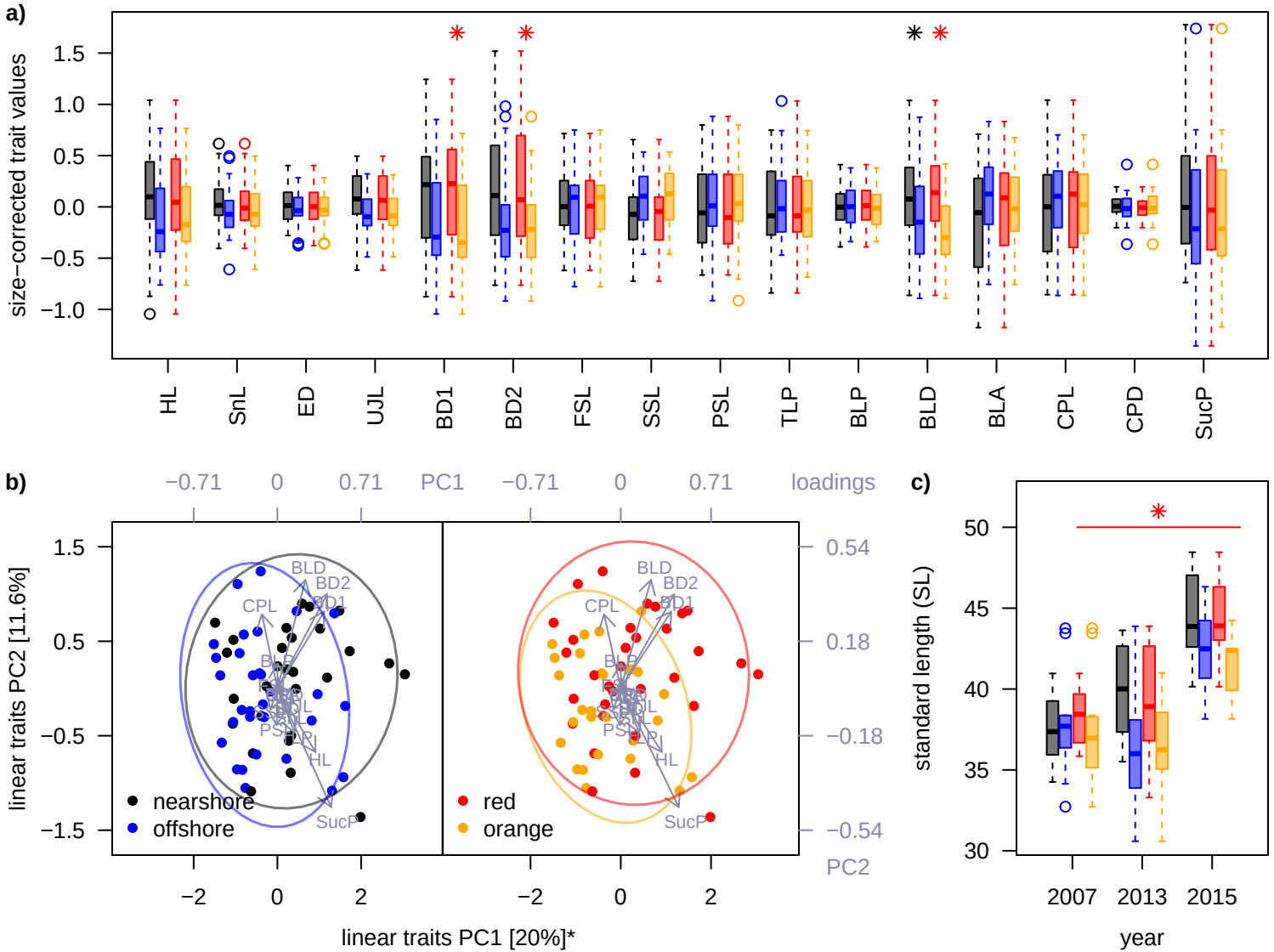
a)
size−corrected trait values
1.5
1.0
0.5
0.0
−0.5
−1.0
HL
SnL
ED
UJL
BD1
BD2
FSL
SSL
PSL
TLP
BLP
BLD
BLA
CPL
CPD
SucP
b)
−0.71
0
0.71
PC1
loadings
0.54
0.18
−0.18
−0.54
PC2
linear traits PC2 [11.6%]
linear traits PC1 [20%]*
nearshore
offshore
red
orange
BLD
BD2
BD1
CPL
BLP
HL
SucP
c)
standard length (SL)
50
45
40
35
30
2007
2013
2015
year

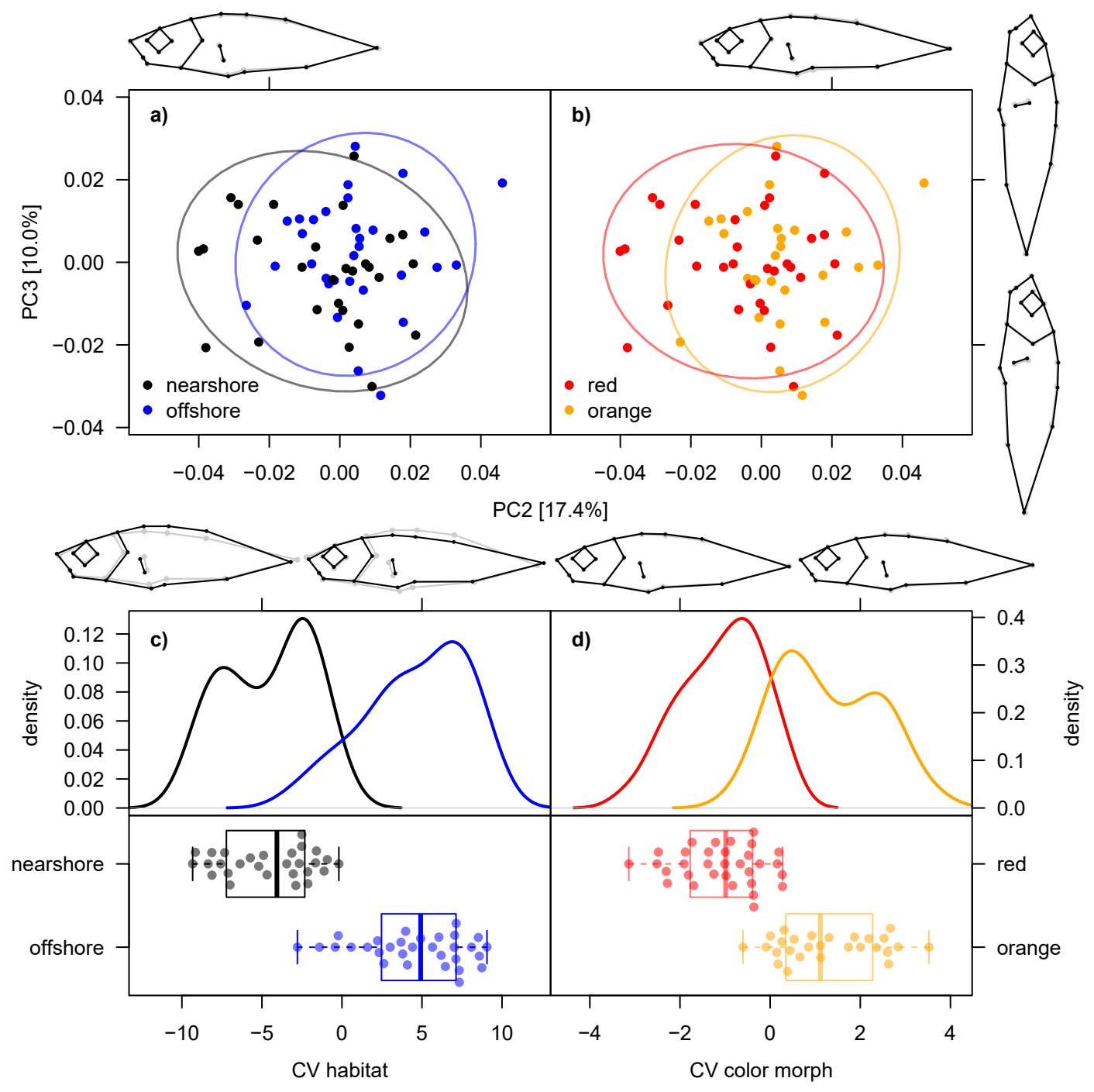
a)
b)
c)
d)
PC3 [10.0%]
PC2 [17.4%]
nearshore
offshore
red
orange
density
CV habitat
CV color morph

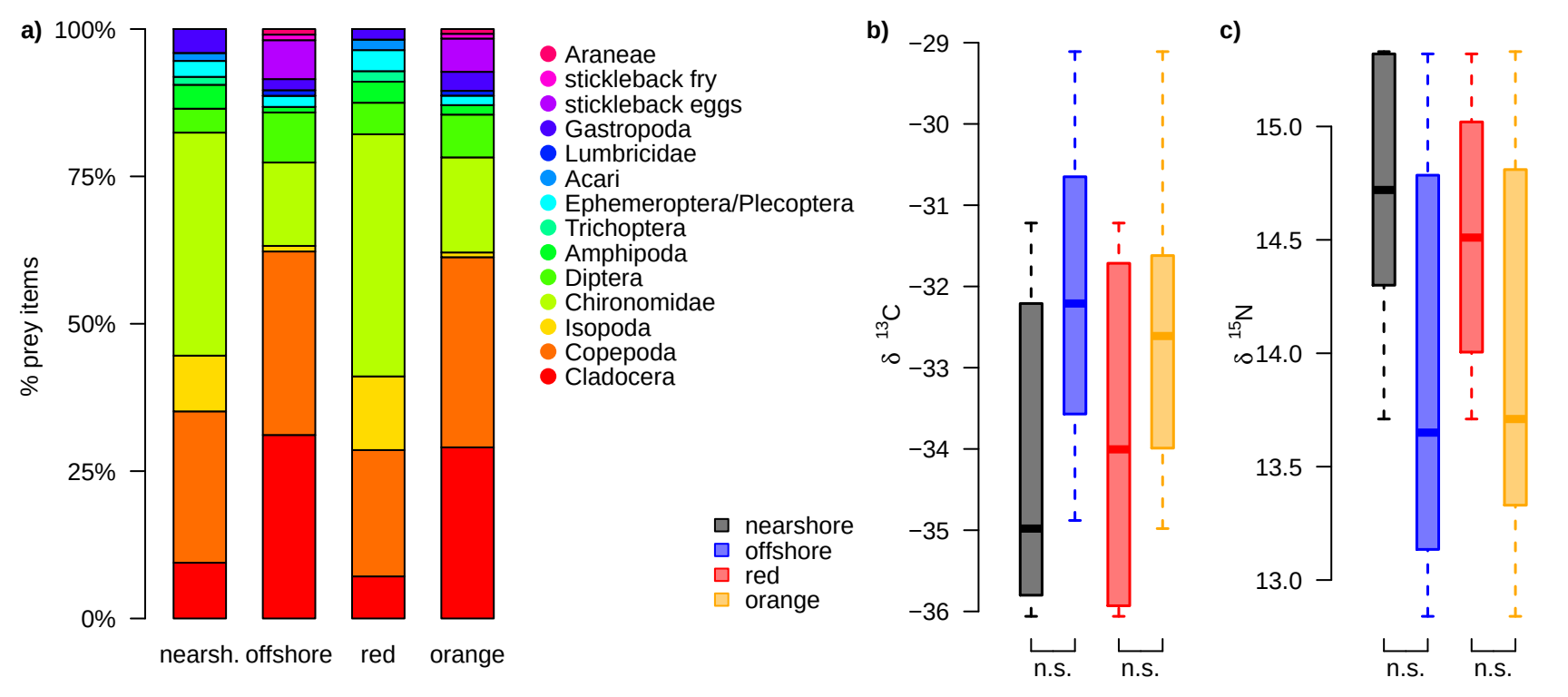
a)
100%
75%
50%
25%
0%
% prey items
nearsh.
offshore
red
orange
Araneae
stickleback fry
stickleback eggs
Gastropoda
Lumbricidae
Acari
Ephemeroptera/Plecoptera
Trichoptera
Amphipoda
Diptera
Chironomidae
Isopoda
Copepoda
Cladocera
nearshore
offshore
red
orange
b)
−29
−30
−31
−32
−33
−34
−35
−36
δ 13C
n.s.
n.s.
c)
15.0
14.5
14.0
13.5
13.0
δ 15N
n.s.
n.s.